AUG 1 7 2000

0830-L-02 NAS 1.29/3-2:00-08

NASA TechBriefs

National Aeronautics and
Space Administration

Electronic Components and Circuits

Electronic Systems

Physical Sciences

Materials

Computer Programs

Mechanics

Machinery

Fabrication Technology

Mathematics and Information Sciences

Life Sciences

00-08

2000-022942/NF C

August 2000

INTRODUCTION

Tech Briefs are short announcements of innovations originating from research and development activities of the National Aeronautics and Space Administration. They emphasize information considered likely to be transferable across industrial, regional, or disciplinary lines and are issued to encourage commercial application.

Availability of NASA Tech Briefs and TSPs

Requests for individual Tech Briefs or for Technical Support Packages (TSPs) announced herein should be addressed to

National Technology Transfer Center
Telephone No. **(800) 678-6882** or via World Wide Web at **www2.nttc.edu/leads/**

Please reference the control numbers appearing at the end of each Tech Brief. Information on NASA's Commercial Technology Team, its documents, and services is also available at the same facility or on the World Wide Web at **www.nctn.hq.nasa.gov**.

Commercial Technology Offices and Patent Counsels are located at NASA field centers to provide technology-transfer access to industrial users. Inquiries can be made by contacting NASA field centers and program offices listed below.

NASA Field Centers and Program Offices

Ames Research Center
Carolina Blake
(650) 604-1754 or
cblake@mail.arc.nasa.gov

Dryden Flight Research Center
Lee Duke
(805) 258-3802 or
lee.duke@dfrc.nasa.gov

Goddard Space Flight Center
George Alcorn
(301) 286-5810 or
galcorn@gsfc.nasa.gov

Jet Propulsion Laboratory
Merle McKenzie
(818) 354-2577 or
merle.mckenzie@jpl.nasa.gov

Johnson Space Center
Hank Davis
(281) 483-0474 or
henry.l.davis1@jsc.nasa.gov

John F. Kennedy Space Center
Gale Allen
(407) 867-6226 or
gale.allen-1@ksc.nasa.gov

Langley Research Center
Sam Morello
(757) 864-6005 or
s.a.morello@larc.nasa.gov

Glenn Research Center
Larry Viterna
(216) 433-3484 or
cto@grc.nasa.gov

George C. Marshall Space Flight Center
Sally Little
(256) 544-4266 or
sally.little@msfc.nasa.gov

John C. Stennis Space Center
Kirk Sharp
(228) 688-1929 or
technology@ssc.nasa.gov

NASA Program Offices
At NASA Headquarters there are seven major program offices that develop and oversee technology projects of potential interest to industry:

Carl Ray
Small Business Innovation Research Program (SBIR) & Small Business Technology Transfer Program (STTR)
(202) 358-4652 or
cray@mail.hq.nasa.gov

Dr. Robert Norwood
Office of Commercial Technology (Code RW)
(202) 358-2320 or
rnorwood@mail.hq.nasa.gov

John Mankins
Office of Space Flight (Code MP)
(202) 358-4659 or
jmankins@mail.hq.nasa.gov

Terry Hertz
Office of Aero-Space Technology (Code RS)
(202) 358-4636 or
thertz@mail.hq.nasa.gov

Glen Mucklow
Office of Space Sciences (Code SM)
(202) 358-2235 or
gmucklow@mail.hq.nasa.gov

Roger Crouch
Office of Microgravity Science Applications (Code U)
(202) 358-0689 or
rcrouch@hq.nasa.gov

Granville Paules
Office of Mission to Planet Earth (Code Y)
(202) 358-0706 or
gpaules@mtpe.hq.nasa.gov

NASA TechBriefs

National Aeronautics and Space Administration

August 2000
00-08

5 Electronic Components and Circuits

11 Electronic Systems

19 Physical Sciences

23 Materials

27 Computer Programs

31 Mechanics

35 Machinery

39 Fabrication Technology

43 Mathematics and Information Sciences

49 Life Sciences

This document was prepared under the sponsorship of the National Aeronautics and Space Administration. Neither the United States Government nor any person acting on behalf of the United States Government assumes any liability resulting from the use of the information contained in this document, or warrants that such use will be free from privately owned rights.

4

BLANK PAGE

Electronic Components and Circuits

Hardware, Techniques, and Processes

7 Supercapacitors With C and Nanostructured MnO_2 Electrodes
8 Efficient Periodic Driving of Piezoelectric Benders
8 Improved Temperature-Compensating Microwave Attenuators
9 Microstrip Patch Rectenna With High Output Voltage

BLANK PAGE

Supercapacitors With C and Nanostructured MnO_2 Electrodes

Energy densities are expected to exceed those of other electrochemical capacitors.

John H. Glenn Research Center, Cleveland, Ohio

A class of developmental asymmetric electrochemical capacitors is based on (1) nonpolarizing positive electrodes made of nanostructured γ-MnO_2, (2) aqueous electrolytes, and (3) polarizing negative electrodes made of activated carbon. Like other state-of-the-art electrochemical capacitors, these can store several hundred times as much energy per unit weight or volume as can traditional electrolytic capacitors. In comparison with other, symmetric state-of-the-art electrochemical capacitors, these asymmetric electrochemical capacitors are expected to be capable of higher energy densities. In addition, by virtue of the high surface areas of the nanostructured γ-MnO_2 electrodes, these capacitors are expected to be capable of high power densities. These capacitors could be particularly useful as load-leveling devices in conjunction with batteries, or as replacements for batteries, in portable electronic devices that rely on short-term intermittent or pulsed high power.

The energy densities of asymmetric electrochemical capacitors can be made to exceed those of symmetric electrochemical capacitors for several reasons:

- The two electrodes of an electrochemical capacitor, having capacitances C_1 and C_2, are electrically connected in series. One of the electrodes is made of a material with a specific charge capacity and thus a capacitance greater than that of the other electrode. The capacitance of the series combination [given by $C_T = C_1C_2/(C_1+C_2)$] is almost equal to the smallest of C_1 or C_2. In contrast, the capacitance of a symmetric electrochemical capacitor is only about half that of either electrode.
- Because the specific charge capacity of one electrode material greatly exceeds that of the other electrode material, the mass and volume of one electrode can be made smaller than that of the other electrode. The decrease in volume translates to an increase in the energy density of the overall capacitor.
- Unlike a symmetric electrochemical capacitor, an asymmetric electrochemical capacitor with an aqueous electrolyte can reliably operate at voltages above 1.22 V without evolution of gas, whereas commercially available symmetric aqueous electrochemical capacitors are limited to about 0.9 V. Inasmuch as energy density is proportional to voltage squared, the energy density of an asymmetric capacitor can be correspondingly higher.

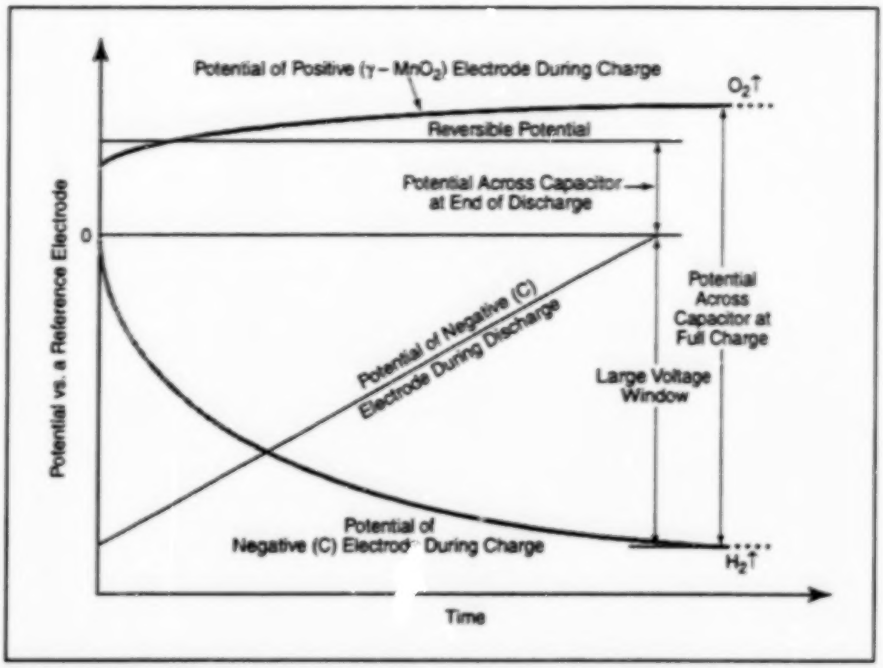
Potential of Positive (γ – MnO2) Electrode During Charge
O2↑
Reversible Potential
Potential Across Capacitor at End of Discharge
0
Potential vs. a Reference Electrode
Potential of Negative (C) Electrode During Discharge
Potential Across Capacitor at Full Charge
Large Voltage Window
Potential of Negative (C) Electrode During Charge
H2↑
Time

A Large Voltage Window is expected to arise through polarization at the negative electrode as a capacitor of the present type is charged. The potential window is limited by the onset of the evolution of hydrogen and oxygen at the electrodes. The potential of the metal oxide electrode remains essentially unchanged during both charge and discharge.

In an asymmetric electrochemical capacitor of the present type, the positive electrode is expected to act as pseudocapacitor: it is expected to store charge through the faradaic reaction

$$\gamma\text{-}MnO_2 + H_2O + e^- \leftrightarrow \alpha\text{-}MnOOH + OH^-$$

with a reversible potential of 1.23 V versus a standard hydrogen electrode. The negative electrode is expected to store charge at the electrode/electrolyte interface (double-layer capacitance).

To make it possible to obtain high energy density, the positive electrode must exhibit a low degree of polarization; that is, the potential of the positive electrode must change little from its reversible potential during the passage of current. In addition, nonfaradaic processes must be minimized and faradaic processes must occur at high reaction rates across the surface of the positive electrode. On the other hand, the negative electrode should be highly polarizable and, under ideal conditions, should develop a large window of potential change during charge and discharge. The figure qualitatively depicts the expected changes in potential at each electrode during charge and discharge.

This work was done by David E. Reisner and T. Danny Xiao of US Nanocorp, Inc.; John R. Miller of JME, Inc.; and Stephen M. Lipka of Florida Atlantic University for **Glenn Research Center**. *Further information is contained in a TSP [see page 1].*

Inquiries concerning rights for the commercial use of this invention should be addressed to NASA Glenn Research Center, Commercial Technology Office, Attn: Steve Fedor, Mail Stop 4–8, 21000 Brookpark Road, Cleveland, Ohio 44135. Refer to LEW-16930.

Efficient Periodic Driving of Piezoelectric Benders

Oscillator driving circuits recover energy during discharges of bender capacitances.

Lyndon B. Johnson Space Center, Houston, Texas

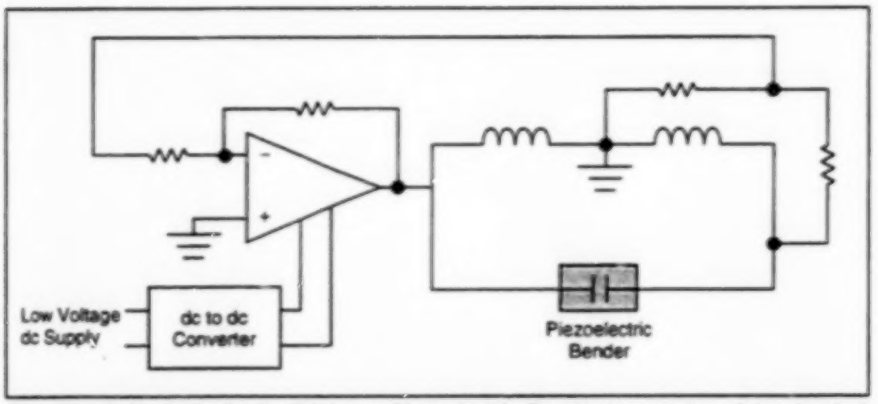

This **Circuit for Periodically Driving a Piezoelectric Bender** is a version of the classical Hartley oscillator.

Modified Hartley oscillator circuits are being developed for use in driving large piezoelectric benders in periodic motion, as in some piezoelectrically driven pumps. These circuits decrease the time-averaged consumption of power and thus increase energy efficiency by recycling large fractions of the energy stored in the capacitances of the piezoelectric benders.

The amount of energy involved is significant because the capacitances of some piezoelectric benders can be large. For example, the capacitance of a system of multilayer piezoelectric benders in one pump has been estimated to be about 160 μF. If all of the energy stored in such a large capacitance during the charge phase of the operating cycle is simply dissipated during the discharge phase, then the time-averaged power consumed is correspondingly large.

An oscillator circuit of the type undergoing development (see figure) can reduce the loss of energy during the discharge phase of the operating cycle when driving a piezoelectric bender. This is because the bender capacitance is the capacitive part of the capacitive/inductive resonant circuit that governs the frequency of oscillation, and by virtue of the fundamental nature of the oscillator circuit, much of the electromagnetic energy handled by this circuit alternates between storage in the capacitance and storage in the inductance. The overall efficiency can be increased if the frequency of mechanical resonance of the pump is matched to the frequency of oscillation.

This work was done by Frank E. Sager and William C. Robertson of Oceaneering Space Systems for **Johnson Space Center**. *Further information is contained in a TSP [see page 1].*

Title to this invention has been waived under the provisions of the National Aeronautics and Space Act [42 U.S.C. 2457(f)], to Oceaneering Space Systems. Inquiries concerning licenses for its commercial development should be addressed to

Oceaneering Space Systems
16665 Space Center Blvd.
Houston, TX 77058-2268

Refer to MSC-22556, volume and number of this NASA Tech Briefs *issue, and the page number.*

Improved Temperature-Compensating Microwave Attenuators

These passive devices feature constant impedances and tailorable temperature coefficients of attenuation.

John H. Glenn Research Center, Cleveland, Ohio

Improved passive temperature-compensating attenuators have been developed for use in processing radio signals at frequencies up to about 18 GHz. In general, temperature-compensating circuits and devices are needed to minimize (preferably, to eliminate) undesired temperature dependences of the overall gains of amplifiers, filters, and other microwave-signal-processing circuits. The role of a temperature-compensating attenuator is to provide a temperature-dependent amount of power dissipation complementary to the temperature-dependent gain or dissipation of other devices in the circuit, such that the overall gain or attenuation of the circuit varies minimally (preferably, not at all) with temperature.

Active temperature-compensating attenuators that include temperature sensors, transistors, and other circuit elements are known; unfortunately, these active attenuators often exhibit nonlinear responses, giving rise to distortion of signals (intermodulation distortion and harmonics). In some applications (e.g., some microwave-signal-processing applications), it is possible to use passive temperature-compensating attenuators, which are preferable to active attenuators in that the passive devices are more reliable and smaller, and their responses to signals are more nearly linear (they do not introduce intermodulation distortion or harmonics).

The improved passive temperature-compensating attenuators were developed because users expressed a need for degrees of temperature compensation greater than those afforded by previously available passive temperature-compensating attenuators. Ideally, in a typical application, a temperature-compensating attenuator intended for use in a specified temperature range would function with no loss (no attenuation) at the highest temperature in the range and with maximum loss at the lowest temperature in the range. While none of the improved attenuators performs in this ideal manner, it is notable that they can be made to present constant input and output impedances, and their temperature coefficients of attenuation (TCAs) are tailorable. Both units with positive and units with negative TCAs have been fabricated.

The improved passive temperature-compensating attenuators are all variants of the same basic device: Each such attenuator comprises a network of thick-film thermistors (similar to thick-film chip resistors) deposited on an alumina substrate. The thermistors are made of materials that have been formulated specifically for this use and that exhibit temperature coefficients of resistance (TCRs) considerably greater than those of previously com-

mercially available materials. The parameters of the thermistors are selected to obtain the desired temperature-dependent amounts of attenuation while maintaining constant input and output impedances.

This work was done by Joseph B. Mazzochette of EMC Technology, LLC for **Glenn Research Center**. *Further information is contained in a TSP [see page 1].*

Inquiries concerning rights for the commercial use of this invention should be addressed to NASA Glenn Research Center, Commercial Technology Office, Attn: Steve Fedor, Mail Stop 4-8, 21000 Brookpark Road, Cleveland, Ohio 44135. Refer to LEW-16927.

Microstrip Patch Rectenna With High Output Voltage

Output voltage is maximized by use of dual polarization and series dc connections.

NASA's Jet Propulsion Laboratory, Pasadena, California

A prototype dual-polarization microstrip patch rectenna dimensioned for an operating frequency of 8.51 GHz has been built to demonstrate a design concept for obtaining maximum output voltage from a rectenna of a given size. This rectenna contains nine square microstrip patch antenna elements in a square array. The antenna can utilize incident radiation with polarization components parallel to either or both sides of the square because the circuitry under each patch includes two independent rectifiers — one for each polarization component. The dc output terminals of the two rectifiers under each patch are connected in series, and the series rectifier pairs of all patches are connected in series. Consequently, the maximum output voltage (obtainable in the special case of circularly polarized incident radiation) can be 18 times that generated by a single-rectifier, single-polarization patch element.

Each microstrip patch antenna element is supported over a ground plane by a layer of lightweight foam with a low (1.07) permittivity. Microstrip feed circuitry, rectifier diodes, and dc conductors that collect the output power are located below the ground plane. Microwave energy is coupled from the antenna elements to the feed circuitry through apertures or coupling slots. Except for this aperture coupling, the antenna and the microstrip feed circuitry are divorced from each other.

The placement of the feed and rectifier circuitry below the ground plane makes it possible to isolate the rectifier circuitry from direct exposure to the incident microwave energy and thus prevents spurious coupling of microwave energy onto the dc conductors. The ground plane also prevents the direct reradiation of the harmonics that are generated by the diodes as unavoidable byproducts of rectification. A microstrip line filter is used to prevent radiation back through the aperture feed. Yet another advantage of mounting the rectifier circuitry below the ground plane is that the ground plane serves as an effective thermal sink for the diodes.

The ground plane is not a single conductive plane but, rather, an array of dc-isolated, capacitively-coupled islands registered with the overlying antenna patches. The capacitive coupling is effected by a thin layer of copper-coated polyimide. The dc isolation of the ground-plane islands in conjunction with the orthogonality of the layout makes it possible to use these islands as parts of the series-connected dc output circuitry.

In tests at an optimized load resistance of 5.4 kΩ, the rectenna was found to function with an overall energy-conversion efficiency exceeding 52 percent over a large range of incident power densities, with a peak of 53 percent at a power density of 38.8 mW/cm^2. The results of the tests also showed that a target output potential of 50 Vdc can be achieved at a power density of 25.2 mW/cm^2.

This work was done by Larry Epp and Abdur Khan of Caltech for **NASA's Jet Propulsion Laboratory**. *Further information is contained in a TSP [see page 1].*

In accordance with Public Law 96-517, the contractor has elected to retain title to this invention. Inquiries concerning rights for its commercial use should be addressed to

Technology Reporting Office
JPL
Mail Stop 122-116
4800 Oak Grove Drive
Pasadena, CA 91109
(818) 354-2240

Refer to NPO-20641, volume and number of this NASA Tech Briefs *issue, and the page number.*

BLANK PAGE

Electronic Systems

Hardware, Techniques, and Processes

13 Adaptive Camouflage
13 Locally Connected Neural Networks for Pattern Recognition
14 Non-Inertial Calibration of Vibratory Gyroscopes
15 Two-Dimensional Active-Pixel Spectral Lidar
16 Acoustic-Emission-Analysis System for Diagnosis of Machinery
17 Cross-Correlated Trellis-Coded Quadrature Modulation
17 Heterodyne Doppler Lidar Using Pseudonoise Code
18 Microfabricated High-Q Optical Resonators for Microphotonics

BLANK PAGE

Adaptive Camouflage

Sensor-and-display systems would create illusions of transparency.

NASA's Jet Propulsion Laboratory, Pasadena, California

Lightweight optoelectronic systems built around advanced image sensors and display panels have been proposed for making selected objects appear nearly transparent and thus effectively invisible. These systems are denoted "adaptive camouflage" because unlike traditional camouflage, they would generate displays that would change in response to changing scenes and lighting conditions.

The basic overall function of an adaptive camouflage system would be to project, on the near side of an object, the scene from the far side of the object. Although adaptive camouflage was conceived for use in battlefield settings (see figure), there are also potential commercial uses — for example, as an electronic "window" that would display a nearby outdoor scene in an office that lacks a real window, or as a home security system in place of a door peephole.

A typical adaptive camouflage system would likely include a network of flexible electronic flat-panel display units arrayed in the form of a blanket that would cover all observable surfaces of an object that one seeks to cloak. Each display panel would contain an active-pixel sensor (APS) [or possibly another advanced image sensor] that would look outward from the panel through an aperture that would occupy only a small fraction of the area of the panel. The blanket would also contain a wiring harness that would include a cross-connected fiber-optic network, through which the image from each APS would be transferred to a complementary display panel on the opposite side of the cloaked object.

The positions and orientations of all the image sensors would be slaved to the position and orientation of one image sensor that would be designated a master imager. The orientations would be determined by a levelling instrument sensed by the master imager. A central controller connected to an external light meter would automatically adjust the brightness levels of all the display panels to make them conform to the to ambient lighting conditions. The underside of the cloaked object would be illuminated artificially so that the display from the top of the cloaked object would show the ground as though in ambient light; if this were not done, then an obvious shadow-induced discontinuity would be seen by an observer looking down from above.

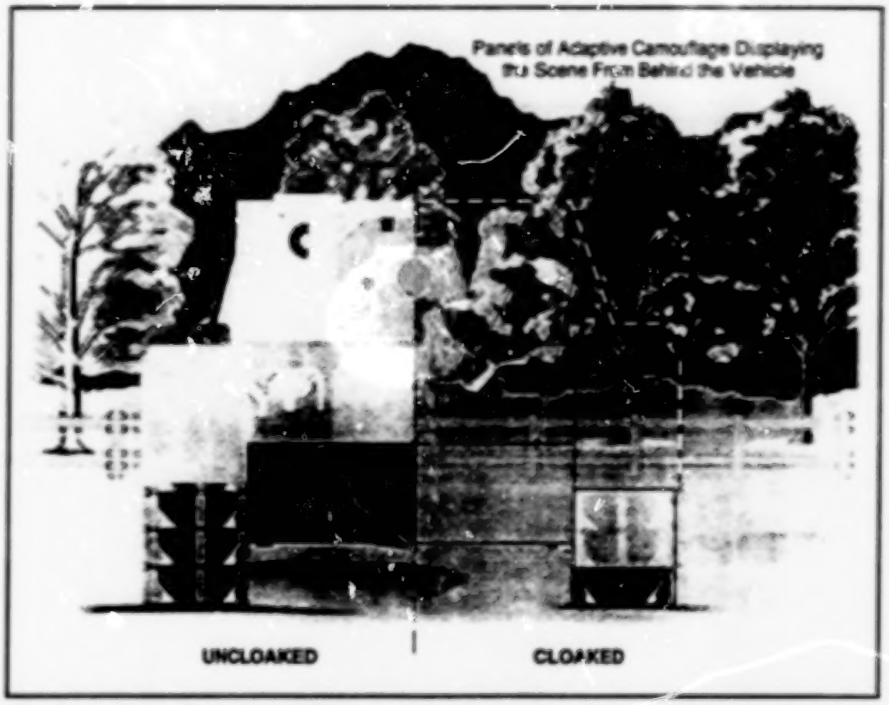

The Scene From Behind an Object would be displayed on panels on the front of the object. The effect of cloaking is illustrated in this simulated image of an armored vehicle with adaptive camouflage on one side only.

The display panels could be sized and configured so that a common inventory of such panels could be used to cloak a variety of objects, without need to modify the objects. Sizes and weights of representative adaptive camouflage systems and subsystems have been estimated: The volume of a typical image sensor would be less than about 1 in.^{3} (≈16 cm^3). A system to completely cloak an object 10 m long by 3 m high by 5 m wide would weigh less than about 100 lb (≈45 kg). If the object to be cloaked were a vehicle, then the adaptive camouflage system could readily be operated on power provided by the vehicle electrical system, without adversely affecting the operation of the vehicle.

This work was done by Philip Moynihan of Caltech and Maurice Langevin of Tracor Round Associates, Ltd., for **NASA's Jet Propulsion Laboratory.** *Further information is contained in a TSP [see page 1].*

NPO-20706

Locally Connected Neural Networks for Pattern Recognition

Patterns could be recognized even if rotated and/or translated.

NASA's Jet Propulsion Laboratory, Pasadena, California

Neural networks of a proposed type would be formed with computational units called "neuromorphs" attached in a locally connected array. These neural networks would achieve pattern recognition invariant under rotation and translation by exploiting a combination of network symmetry and biologically inspired image-information-processing concepts. The architecture of these networks can be implemented in software; it is also suitable for implementation in hardware in the form of single-chip integrated circuits that would function in parallel-processing modes and thus be capable of fast recognition of patterns.

A typical previously developed image-recognition system effects a process that includes a feature-extraction subprocess fol-

lowed by a classification subprocess: First, the system extracts features relevant to the kinds of objects that it seeks to classify. These features tend to fall into three classes: global, local, and relational. These feature vectors are then put into a classifier that has been trained or structured to differentiate the feature vectors into different pattern groups.

A neural network of the proposed type would produce feature vectors that would be global, local, and relational, all at the same time. Consequently, for some applications, single feature vectors would be all that would be needed for classification; moreover, inasmuch as features would be easily differentiable, adequate back-end classifier subsystems could be made less complex than those of previously developed pattern-recognition systems. The proposed neural networks could be made quite compact and suitable for analog array processing systems in which neuromorphs would be incorporated directly into the electronic circuitry of image-detecting arrays of photodetectors. Eventually, efforts to integrate this type of neural pattern-recognition circuitry with image-sensing circuitry should lead to the development of single chips that would perform image-acquisition and pattern-recognition functions analogous to visual preprocessing in eye/brain systems.

The concept of a locally connected network of neuromorphs evolved from previous research on the use of pulse-coupled neural networks for fast, invariant automatic target recognition. More specifically, the proposed network architecture is derived from, but is more efficient than, the architecture of an experimental pattern-recognition neural network based on a biomorphic neuron model that includes both the spiking behavior at the axon hillock and the synapto-dendritic processing of a biological neuron. The proposed neural networks would process information in a manner similar to that of the pulse-coupled neural networks, but could be implemented more easily and could process information at higher rates.

The results of computational simulations of the architecture of the proposed systems indicate an ability to perform translation- and rotation-invariant pattern recognition. Analog integrated circuits for use as building blocks (neuromorphs) of locally connected neural networks of the proposed type were designed and tested in other computational simulations, and the results of these simulations indicate that in comparison with previously developed pattern-recognition systems, the proposed system could achieve faster convergence, could operate with lower power consumption, and could be fabricated with greater integration density.

This work was done by Tyson Thomas of Caltech for **NASA's Jet Propulsion Laboratory**. *Further information is contained in a TSP [see page 1].*

This invention is owned by NASA, and a patent application has been filed. Inquiries concerning nonexclusive or exclusive license for its commercial development should be addressed to the Patent Counsel, NASA Resident Office–JPL [see page 1]. Refer to NPO-20633.

Non-Inertial Calibration of Vibratory Gyroscopes

Coriolis forces would be simulated by electrostatic forces.

NASA's Jet Propulsion Laboratory, Pasadena, California

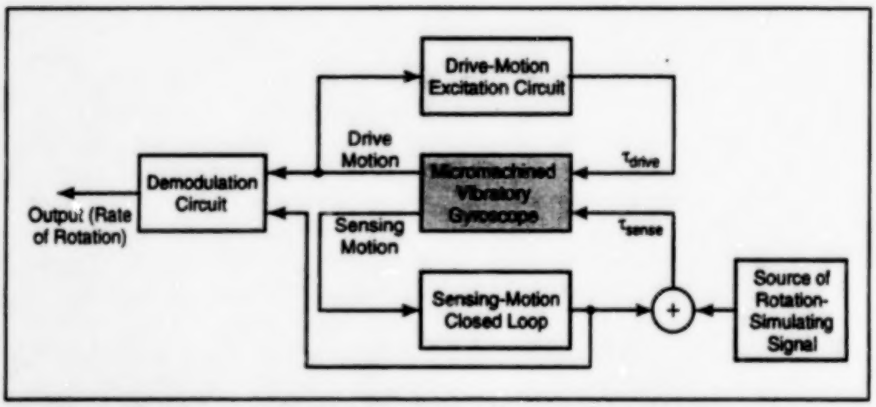

The Effect of Rotation would be simulated electronically by injecting a signal that would generate an electrostatic force to mimic the Coriolis force.

A proposed method of calibration of micromachined vibratory gyroscopes would make it unnecessary to test the gyroscopes at known rates of rotation. At present, calibration entails inertial tests in which the gyroscopes are exposed to tumble and rotation maneuvers on multi-axis precise rotation tables, which are expensive. By eliminating the need for the rotation tables, the proposed method could reduce the cost of calibration. Moreover, inasmuch as the number of gyroscopes that a rotation table can hold is limited, the elimination of rotation tables method would make it possible to test more gyroscopes simultaneously.

The proposed method is based on the unique principle of operation of a micromachined vibratory microscope. This principle involves electrostatic excitation, capacitive sensing, and feedback control of vibrations of a microscopic body designed so that its vibrational modes are affected by the Coriolis force. One of the feedback control signals is a negative feedback signal for generating an electrostatic actuation force that compensates for the Coriolis force. In the proposed method, one would superimpose a simulated Coriolis-force signal on the electrostatic actuation signal.

Because signals representing the real and simulated Coriolis forces would be at the same frequency and phase, the gyroscope circuitry would respond to the simulated Coriolis force in the same way in which it would respond to the real Coriolis force. Hence, rotational testing would not be necessary because one could simply inject the simulated Coriolis-force signal into the feedback control loop to make the vibrations and the associated electronic signals behave as though the gyroscope were undergoing rotation.

The figure is a block diagram of an electronic system for implementing the method. The drive-motion excitation circuit would measure the drive motion (one of two vibratory motions involved in the basic principle of operation) and would provide an excitation force to sustain this motion. The sensing-motion closed loop would provide electrical damping of the sensing motion (the other vibratory motion involved in the basic principle of operation). The feedback control signal, τ_{sense}, would produce an electrostatic actuation force equal to the real Coriolis force plus the simulated (rotation-simulating) Coriolis force. The demodulation circuit would demodulate a sensing-motion force-rebalancing signal with the drive-motion signal to generate a signal proportional to the

rate of rotation. During the simulation of rotation, the sensing-motion closed loop and the demodulation circuit would respond as though to a real rotation signal.

Of course, the value of this method of calibration would depend on the accuracy with which the simulated Coriolis-force signals could be made to duplicate the effects of the real Coriolis force. It would be necessary to perform conventional inertial calibration to verify the proposed method.

This work was done by Roman Gutierrez and Tony K. Tang of Caltech for **NASA's Jet Propulsion Laboratory**. *Further information is contained in a TSP [see page 1].*

In accordance with Public Law 96-517, the contractor has elected to retain title to this invention. Inquiries concerning rights for its commercial use should be addressed to

Technology Reporting Office
JPL
Mail Stop 122-116
4800 Oak Grove Drive
Pasadena, CA 91109
(818) 354-2240

Refer to NPO-20659, volume and number of this NASA Tech Briefs issue, and the page number.

Two-Dimensional Active-Pixel Spectral Lidar

Targets would be probed using spatially, temporally, and spectrally resolved optical signals.

NASA's Jet Propulsion Laboratory, Pasadena, California

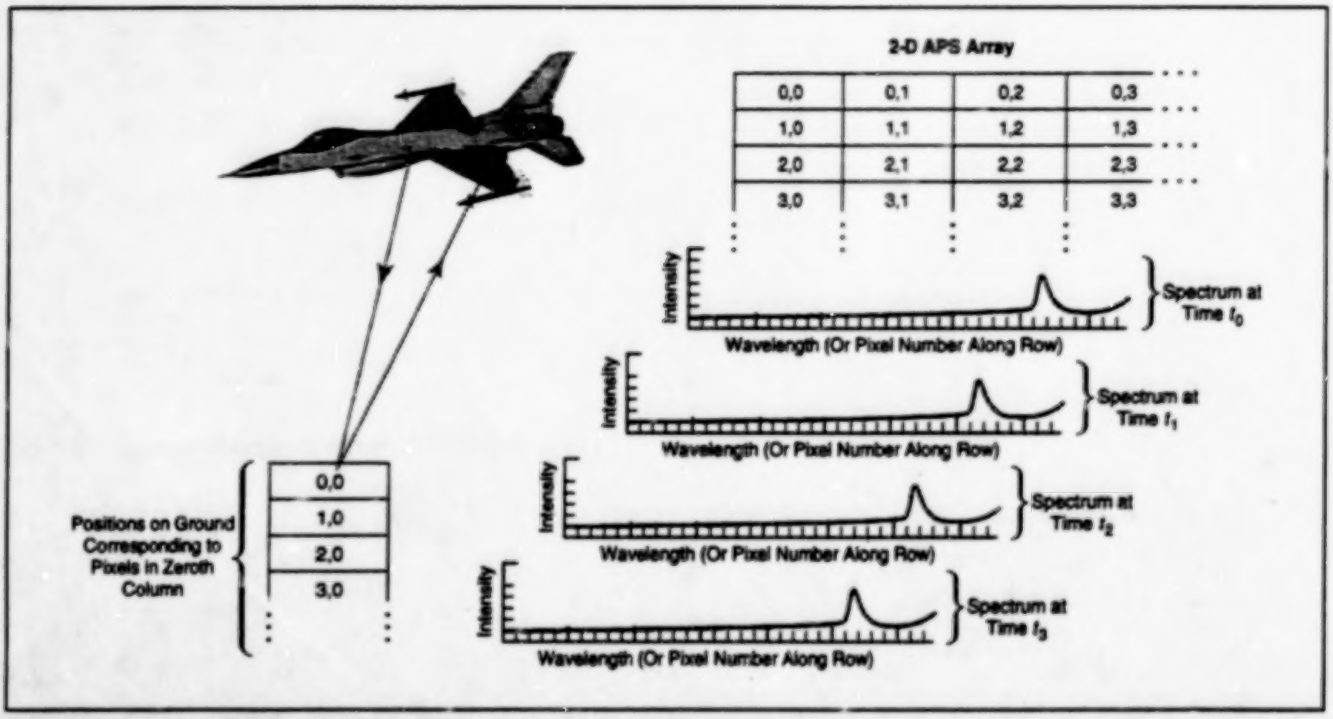

Light Returning from the Target Would Be Spectrally Dispersed — in this case, along the zeroth row of an APS array. Hence, by processing the readouts from the pixels in this row at different times, one could obtain a time-resolved spectrum of the target.

Two-dimensional active-pixel-spectral lidar (TAPSL) is a proposed remote-sensing technique for obtaining spatially, spectrally, and temporally resolved information about terrain or other targets. Operating aboard an airborne or spaceborne platform above the Earth or a remote planet, a TAPSL system would be used to gather data on geological, biological, and chemical phenomena that manifest themselves through characteristic optical emission spectra.

A TAPSL system would include a single-frequency laser that would illuminate a target. The light returning from the target would include an elastically scattered component (the spectral component at the original laser frequency) that could be used for ranging as in conventional lidar. The return would also include inelastically scattered (Raman-shifted and fluorescent) spectral components that would be characteristic of the target material in response to excitation by the laser.

The light returning from the target would be detected by a rectangular array of active-pixel sensors (APSs) that would be sensitive to visible and near-infrared light. The APS would operate in conjunction with miniaturized electronic control, readout, and pixel-data-processing circuits. Before impinging on the APS array, the light would pass through a diffraction grating oriented to disperse the light along the rows of pixels. Consequently, the frequency or wavelength of the light received by each pixel could be identified from the position of the pixel along its row (see figure). Optionally, the system could be operated without the laser to obtain the reflected-sunlight spectrum and/or the thermal spectrum of the target.

As described thus far, the system would derive information about the relative position of the target in the manner of conventional lidar. However, if a lens were used to image the target scene onto the APS, then the position of each pixel along a column could be used to obtain spatial resolution along the corresponding axis on the target; this approach could be useful if the laser beam did not provide sufficient resolution, or if it were desired to scan the terrain in "pushbroom" fashion. Alternatively, it might be possible to vary the time gate of each pixel with position along each column to obtain additional resolution for ranging or spectral analysis.

This work was done by Quisup Kim of Caltech for **NASA's Jet Propulsion Laboratory**. *Further information is contained in a TSP [see page 1].*

NPO-20737

Acoustic-Emission-Analysis System for Diagnosis of Machinery

High-frequency acoustic signals are processed to extract indications of bearing defects.

Marshall Space Flight Center, Alabama

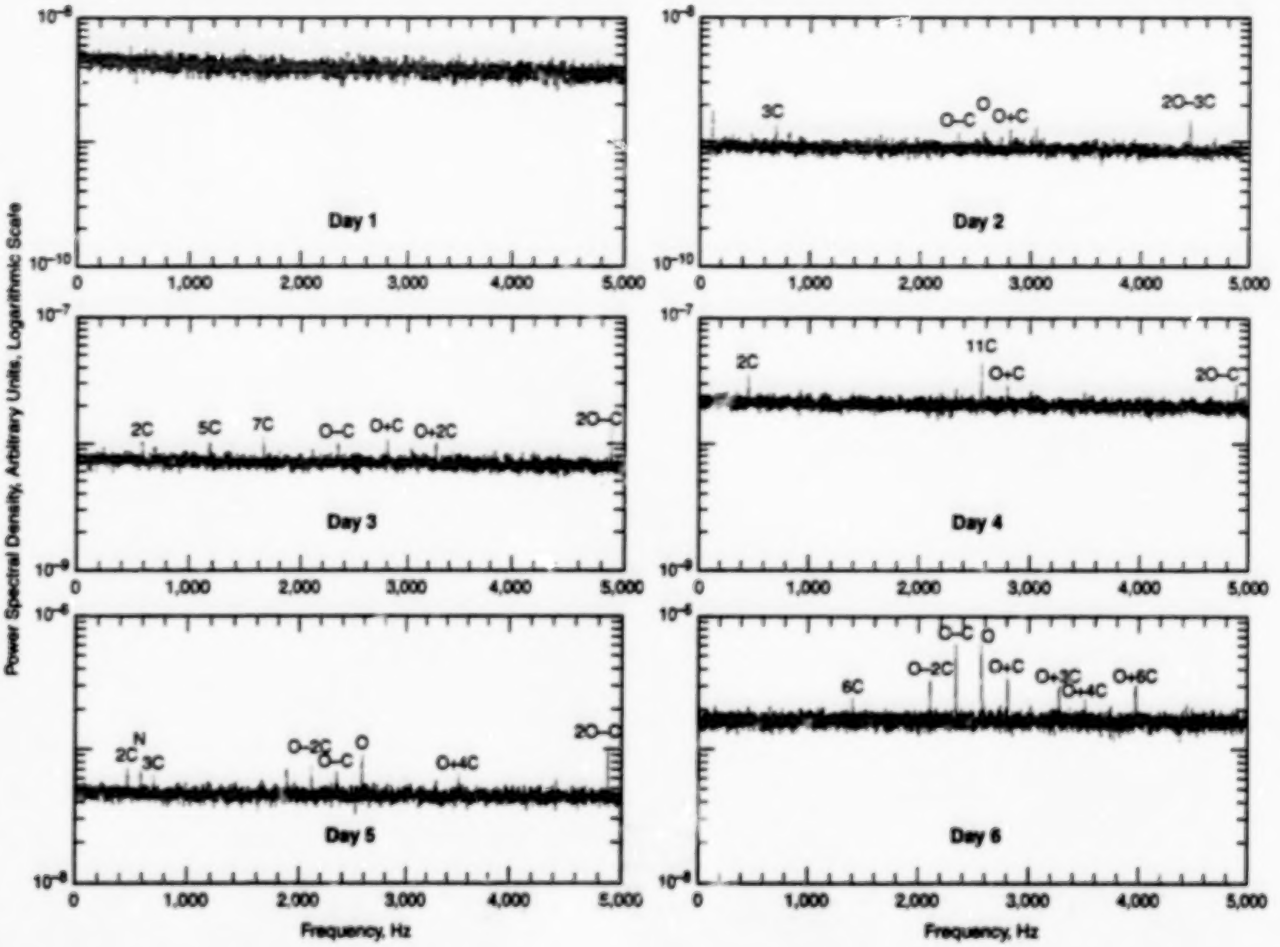

These AE Envelope Power Spectral Distributions were obtained in tests of a ball bearing. Even though the acoustic sensor did not sense low-frequency phenomena directly, the envelope analysis extracted low-frequency bearing information from the high-frequency sensor output. The succession of plots shows a wear trend in the bearing signature. The symbols "O" and "C" (some preceded by integers) signify the outer-race frequency and cage frequency (or a harmonic thereof), respectively. Combinations of "O" and "C" signify modulation products of the indicated frequencies. "N" signifies the shaft rotation frequency.

A personal-computer-based system has been developed as a prototype of electronic signal-processing and computing systems for diagnosis of turbines, motors, and other rotary machines through analysis of acoustic emissions. The system includes acoustic sensors that respond in the kilohertz-to-megahertz frequency range wherein acoustic energy tends to emanate from bearing defects. The system also includes a relatively inexpensive desktop computer and a 12-bit analog-to-digital converter that can acquire acoustic-sensor readings in as many as four channels at a sampling rate up to 5 MHz per channel.

The reason for choosing the kilohertz-to-megahertz frequency range is that when the digitized acoustic-emission (AE) signals in this frequency range are processed by suitable algorithms to obtain indications of deterioration of bearings, the resulting indications are more reliable than are those obtained by similar processing of the outputs of accelerometers that sense lower-frequency vibrations. The algorithms in question implement envelope analysis (see figure) and another signal-processing technique called "point process spectral analysis" (PPSA).

In a typical application, vibration sources other than a defective bearing that one seeks to diagnose can be expected to give rise to a variety of anomalous transient events, including random spikes, in the AE signal. These anomalous transient events can mask bearing signatures and prevent reliable detection of bearing faults. A common obstacle encountered in analyzing an AE signal is the inability to determine which transient events are related to shaft rotation and which are not. Conventional time-series and spectral analyses are ineffective in distinguishing between useful and useless signal features. In addition, a bearing defect in its early stage generates intermittent transient impulses with weak periodicities. It is difficult to detect these periodicities through conventional envelope spectral analysis. Furthermore, the need to process a high-frequency AE signal in real time imposes a severe computational requirement, which constitutes an impedi-

ment to the design of an inexpensive bearing-diagnostic system.

PPSA was summarized in "Acoustic-Emission Bearing-Fault Diagnosis System" (MFS-26468), *NASA Tech Briefs*, Vol. 21, No. 11 (November 1997), page 84. PPSA provides high computational efficiency in the spectral analysis of transient events in a high-frequency AE signal. In turn, this computational efficiency enables the prototype bearing-diagnostic system to operate with a minimal processing gap (time delay), so that it can generate diagnostic indications in nearly real time. When pulses from sources other than a defective bearing corrupt the bearing-generated transient pulses, PPSA can provide a detection-and-discrimination capability superior to that of envelope analysis.

The prototype bearing-diagnostic system is programmed with an additional post-test vibration-signal-analysis software package called "PC-SIGNAL." This software is effective and easy to use for general applications in analysis of vibrations, monitoring the "health" of machinery, and diagnosis of faults. PC-SIGNAL also includes a number of subprograms designed especially for processing high-frequency AE signals.

This work was done by Jen-Yi Jong of AI Signal Research, Inc., for **Marshall Space Flight Center**. *For further information, please contact the company at* ***www.aisignal.com*** *or (256) 551-0008.*

Inquiries concerning rights for the commercial use of this invention should be addressed to the Patent Counsel, Marshall Space Flight Center [see page 1]. Refer to MFS-31468.

Cross-Correlated Trellis-Coded Quadrature Modulation

There is more flexibility for optimization than there is in older related modulation techniques.

NASA's Jet Propulsion Laboratory, Pasadena, California

Cross-correlated trellis-coded quadrature modulation (XTCQM) has been proposed as a generic scheme with specific embodiments that potentially offer superior alternatives to other highly power- and bandwidth-efficient phase-shift-keying (PSK) modulation schemes. Examples of such schemes include Gaussian minimum-shift keying (GMSK), staggered quadrature offset raised cosine (SQORC), Feher's patented quadrature PSK (FQPSK), and pulse-shaped offset quadrature PSK (OQPSK).

Previously developed trellis-coded-modulation (TCM) techniques combine (1) the bandwidth efficiency of such conventional multilevel-modulation techniques as multiple-phase-shift keying (MPSK) and quadrature amplitude modulation (QAM) with (2) the power efficiency of error-correction coding into (3) unified modulation schemes that, through suitable mappings, simultaneously exploit the desirable properties of (1) and (2). While the previously developed TCM techniques afford the bandwidth efficiency inherent in multilevel modulation, less attention was given, in the development of those techniques, to achieving high levels of spectral containment as quantified, for example, by keeping out-of-band power levels low to minimize adjacent-channel interference.

Considering only quadrature modulations, the innovative aspect of the development of XTCQM lies in a focus on the spectral occupancy of the transmitted signal, along with careful attention to a desirable constant-envelope property and to the power efficiency of the demodulation/decoding operation at the receiver. The more-generic nature of XTCQM (as compared with FQPSK and other schemes) affords considerably more flexibility for trading off between power and spectral efficiencies.

In XTCQM, a cross-correlation and a suitable waveform mapping are introduced into the in-phase (I) and quadrature (Q) baseband signals transmitted on quadrature carriers, in such a way as to provide a high level of spectral efficiency while also maintaining high power efficiency and a constant or pseudo-constant envelope. XTCQM would be implemented by use of such standard, currently available subsystems as an offset-QPSK modulator and a receiver containing such items as matched filters, and a Viterbi decoder. The transmitter portion of a conceptual XTCQM communication system has been shown, in a computational simulation, to perform as predicted by theory. At the time of reporting the information for this article, the software for computational simulation of the performance of the receiver portion of the system was in an early stage of development.

This work was done by Marvin K. Simon and Tsun-Yee Yan of Caltech for **NASA's Jet Propulsion Laboratory**. *Further information is contained in a TSP [see page 1].*

NPO-20532

Heterodyne Doppler Lidar Using Pseudonoise Code

This low-power, compact unit will be suited to a variety of meteorological uses.

NASA's Jet Propulsion Laboratory, Pasadena, California

A low-power, miniature Doppler lidar instrument is being developed for use in measuring opacity (from dust) and wind profiles in the Martian atmosphere. The instrument could also be used on Earth to measure turbulence in the atmospheric boundary layer, for assessments of urban and regional air quality, and, perhaps for studying aircraft wing-tip vortices. The instrument is being designed to measure wind velocity component along its line of sight with a precision of 1 m/s and to perform ranging at distances from 3 km to a maximum of 10 km (or less, depending on the concentration of airborne dust).

There are other Doppler lidar systems that produce range-gated measurements of opacity and wind velocities, but those systems are unacceptably large and power-hungry for the intended application. The other systems contain, variously, gas or solid-state lasers operating in pulse mode. The heart of the transmitter in the present developmental instrument is a diode laser, which is chosen for compactness and because the electrical efficiencies of diode lasers are generally greater than those of gas and solid-state lasers. On the other hand, diode lasers are not suitable for pulsed operation at the peak power levels and pulse-repetition frequencies needed for range gating in the intended application; therefore, in the present instrument, range gating is achieved by use of a

pseudonoise code.

The instrument will be highly electrically efficient. The diode laser in the transmitter will operate with a conversion efficiency approaching 40 percent. The design of the instrument will incorporate recent developments in high-speed, low-power receiver electronics.

The transmitting diode laser will be modulated with the pseudonoise code — a prescribed pseudorandom sequence of "on" and "off" states — with each "on" or "off" state lasting 1 to 2 μs. The receiver will perform heterodyne detection; it will include a beam splitter, which will enable the use of a local-oscillator diode laser modulated and frequency-shifted (to measure the Doppler effect) separately from the transmitting diode laser. The entire transmitter/local-oscillator package will be compatible with fiber optics.

For the original Mars-wind-profiling application, the desired transmitter power is about 200 mW. The spectral width of the transmitted light must be no more than about 1 MHz. At present, these requirements can be satisfied by use of a diode laser master oscillator and a fiber laser amplifier, and compact diode-laser devices that satisfy these requirements are expected to be developed during the next few years.

The receiver will include a unique, high-speed, low-noise photomixer with a matched amplifier and a high-speed, low-power, 12-bit analog-to-digital converter followed by circuitry that computes fast Fourier transforms and circuitry that processes power spectra.

This work was done by Robert Menzies, Greg Cardell, and Hamid Hemmati of Caltech for **NASA's Jet Propulsion Laboratory**. *Further information is contained in a TSP [see page 1].*
NPO-20466

Microfabricated High-*Q* Optical Resonators for Microphotonics

Ultra-high-*Q* microcavities would be mass-produced and integrated by techniques adapted from microelectronics.

NASA's Jet Propulsion Laboratory, Pasadena, California

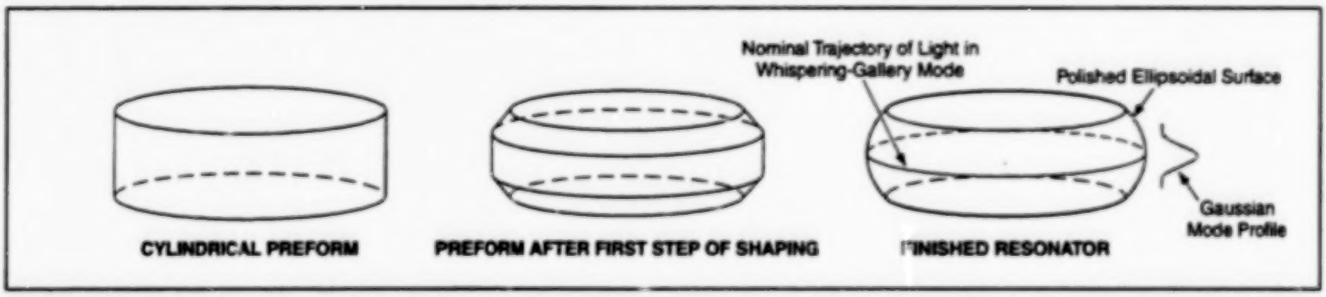

An Ellipsoidal Optical Resonator would be fabricated by micromachining, starting from a preform of fused silica or other highly-transparent material.

Submillimeter-sized, transparent, solid, truncated spheres and ellipsoids for use as optical resonators in integrated microphotonic devices would be made by microfabrication techniques like those used in the electronic industry to make integrated circuits, according to a proposal. Such resonators, heretofore denoted generally as "microspheres," have been described in several recent articles in *NASA Tech Briefs*. In a microsphere, resonance is achieved through glancing-incidence total internal reflection in one or more "whispering-gallery" modes, in which the light propagates in equatorial planes near the surface, with an integer number of wavelengths along a nominal closed circumferential trajectory. If the surface of the resonator is sufficiently smooth and a sufficiently close approximation of a sphere or ellipsoid, then in principle, the resonance quality factor (Q) is limited only by attenuation in the resonator material; for a microsphere made of fused silica, this translates to a potential to obtain $Q \geq 10^{10}$.

Heretofore, microspheres have been fabricated manually, in small numbers, for use in laboratory experiments. The proposal regarding adaptation of microfabrication techniques is prompted by a desire to obtain mass-producibility of such resonators with reproducibility of design, plus a capability for integration of the resonators with other photonic devices.

A typical fabrication sequence according to the proposal (see figure) would begin with preparation of a circular cylindrical disk preform of the resonator material, with a diameter between 100 and 200 μm and an axial thickness of 20 to 40 μm. Chamfers would be introduced at the top and bottom edges, and the resulting edges would be chamfered further, so that the original cylindrical surface would be made to evolve toward an ellipsoid. This shaping would be accomplished in a sequence of steps that could include a combination of thermal and mechanical treatments. Alternatively, shaping could involve wet and/or dry etching, ion milling, laser-assisted etching, chemical-assisted ion-beam etching, and/or other processes.

In the final steps of fabrication, the remaining edges would be rounded and the ellipsoidal surface smoothed to minimize roughness and thereby reduce the scattering loss of light. Final treatment could include radiative heating to fire-polish the surface to reduce the surface roughness to the subnanometer level (in effect, the molecular level).

The finished resonator would have an ellipsoidal surface near the plane of symmetry. Because of the nearly Gaussian falloff of the whispering-gallery modes away from their localization near the symmetry plane, the truncated ellipsoid would be electromagnetically indistinguishable from a full ellipsoid. Consequently, flat border surfaces could be used for mounting or heat-sinking without adverse effect on the performance of the optical cavity.

This work was done by Vladimir Iltchenko and Chi Wu of Caltech for **NASA's Jet Propulsion Laboratory**. *Further information is contained in a TSP [see page 1].*
NPO-20604

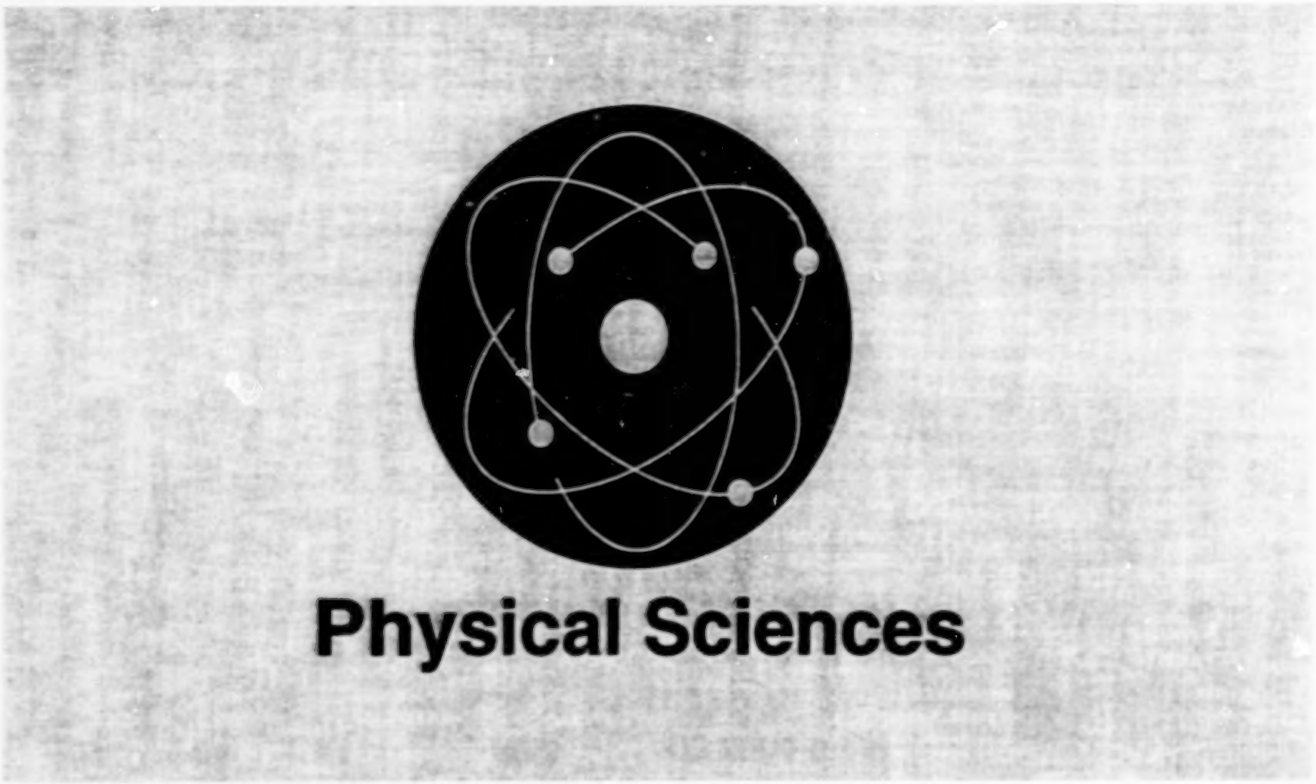

Physical Sciences

Hardware, Techniques, and Processes

21 Atmospheric Electron X-Ray Spectrometer

21 Software for Designing Model Rockets for Base-Heating Tests

BLANK PAGE

Atmospheric Electron X-Ray Spectrometer

Specimen surfaces can be analyzed quickly, at high spatial resolution.

NASA's Jet Propulsion Laboratory, Pasadena, California

The Atmospheric Electron X-ray Spectrometer (AEXS) is being developed for performing rapid, nondestructive *in situ* analyses of the elemental composition of surfaces. The capability of the AEXS to operate in air and to be brought to a surface to be analyzed makes it unnecessary to bring a specimen to a laboratory and prepare the specimen for analysis.

The AEXS belongs to a class of miniature instruments that perform *in situ* elemental composition analysis by the excitation and analysis of x-ray fluorescence from specimens. Prior techniques include excitation of the x-ray fluorescence by α particles and x rays, both of which entail larger target areas and longer spectrum acquisition times than the electron beam based excitation used in the AEXS. The AEXS is predicted to be able to analyze samples at high spatial resolution determined by its controllable electron-beam spot size. The spectrum acquisition time of the AEXS is expected to be less than a minute. The short spectrum acquisition time results in less energy consumption and makes the AEXS suitable for incorporation into manufacturing, inspection, and quality control processes.

The figure schematically depicts a laboratory prototype of a portable AEXS instrument. Electrons are generated, accelerated, and focused by a commercially available electron gun within an evacuated enclosure. The vacuum is isolated from the ambient atmosphere by an electron-transparent membrane. The membrane is microfabricated from low-atomic-number materials such as silicon nitride, boron nitride, or diamond. Active pumping of the electron column against leaks and diffusion of air through the membrane can be achieved by an ion pump.

The electron beam passes through the membrane and travels a short distance to the specimen surface. The electrons impinge on the surface, exciting x rays at wavelengths characteristic of surface elements. The x rays are detected by a thermoelectrically cooled silicon positive/intrinsic/negative (PIN) photodiode. The signal from the PIN photodiode is fed into a signal-conditioning amplifier and a multichannel analyzer. The output of the multichannel analyzer is an x-ray spectrum that can be analyzed to determine the elemental composition of the surface.

The instrument is designed to be powered by a battery. The high voltage (30 kV) for the electron gun is generated by a miniature voltage multiplier circuit. Instrument control electronics are required to operate the electron gun, ion pump, x-ray detector, and analyzer. The spectrum from the multichannel analyzer is routed through a serial interface to a computer.

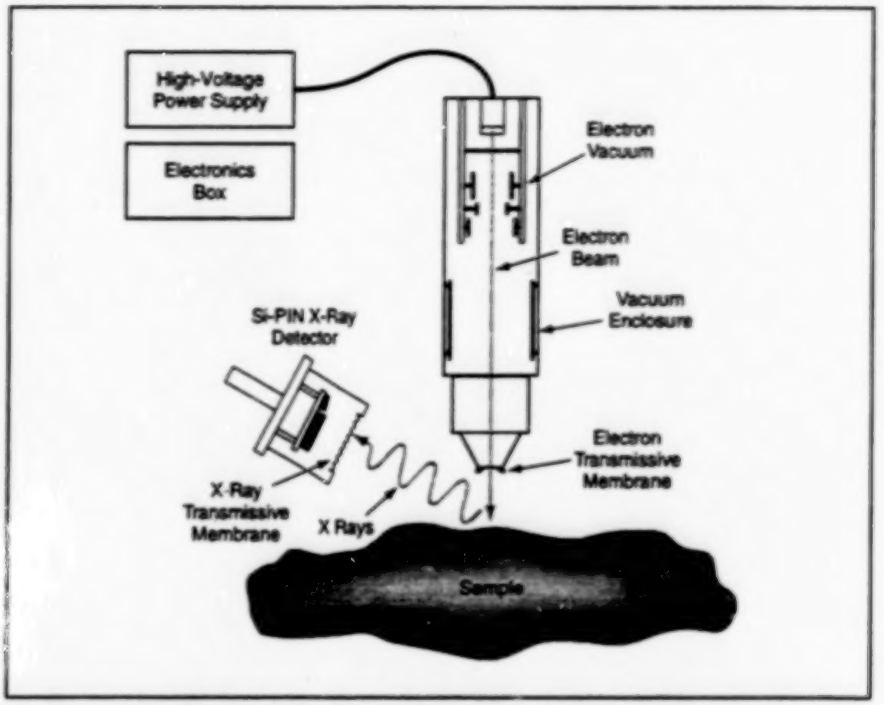

An Atmospheric Electron X-Ray Spectrometer shown in this schematic is designed to be a portable instrument that can be brought to a specimen surface. After operation of about a minute, it can give information on the elemental composition of the specimen surface. The dimensions of the instrument in its final form are expected to be about 4 by 8 by 14 in. (about 10 by 20 by 36 cm).

This work was done by Jason Feldman, Thomas George, and Jaroslava Wilcox of Caltech for **NASA's Jet Propulsion Laboratory**. *Further information is contained in a TSP [see page 1].*

In accordance with Public Law 96-517, the contractor has elected to retain title to this invention. Inquiries concerning rights for its commercial use should be addressed to

Technology Reporting Office
JPL
Mail Stop 122-116
4800 Oak Grove Drive
Pasadena, CA 91109
(818) 354-2240

Refer to NPO-20463, volume and number of this NASA Tech Briefs *issue, and the page number.*

Software for Designing Model Rockets for Base-Heating Tests

This program eliminates a week or more of manual calculations for each configuration.

Marshall Space Flight Center, Alabama

The Impulse Combustion Excel (ICE) computer program was developed to facilitate and accelerate the design and analysis of subscale rocket engines for use in base-heating tests. Such tests are performed on the ground to obtain data for estimating the heating effects of hot exhaust plumes on the aft regions of full-scale rockets during ascent. The comput-

er program is so named because typically, a base-heating test involves impulse combustion — short-duration (of the order of 100 ms long) hot firing using flight propellants. Heretofore, the design of the subscale engines and base-heating tests has been a difficult, time-consuming, iterative process. ICE can be expected to reduce the testing times and costs and to yield improved designs. ICE can be used to design models to be tested in both wind tunnels and vacuum tanks.

ICE is a spreadsheet code that provides all of the parametric data used in the geometric design, heating analysis, and system analysis for many propulsion systems. The power of ICE lies in the capability to change only one or all input variables to adjust a design. ICE can also be used as an educational tool for learning the effects of various parameters on an entire design.

ICE eliminates a week or more of manual calculations for each model configuration. The program incorporates engineering relations that have been used previously but, until now, have been found in several reports and documents and never gathered into one consistent form or location. In addition, ICE incorporates an expanded set of features including (1) a procedure for determining the loss of energy resulting from internal transfer of heat to cold metal surfaces, (2) a methodology for sizing a combustion chamber and associated ports of one or more engine(s), (3) a valve-selection sheet, and a (4) historical design data base.

The spreadsheet contains the following pages: (1) input, (2) Venturi sizing, (3) charge-tube and buffer-gas-tube lengths, (4) system start time, (5) injector design, (6) combustor design, (7) combustor/nozzle heating, (8) surface heating, (9) valve pressure drop, and (10) historical design data. When the input page is filled out, ICE automatically generates the specifications necessary for computer-aided design (CAD) of a model. The CAD numerical model can be translated into an image of a solid model for electronic display and visual inspection; alternatively or in addition, a material model can be grown from the numerical model by use of stereolithography.

This work was done by Carl D. Engel of Qualis Corp. for **Marshall Space Flight Center**. *For additional information, please contact the company at (256) 533-9282.*

In accordance with Public Law 96-517, the contractor has elected to retain title to this invention. Inquiries concerning rights for its commercial use should be addressed to

Qualis Corporation
3225 Bob Wallace Ave.
Suite C
Huntsville, AL 35805

Refer to MFS-31402, volume and number of this NASA Tech Briefs *issue, and the page number.*

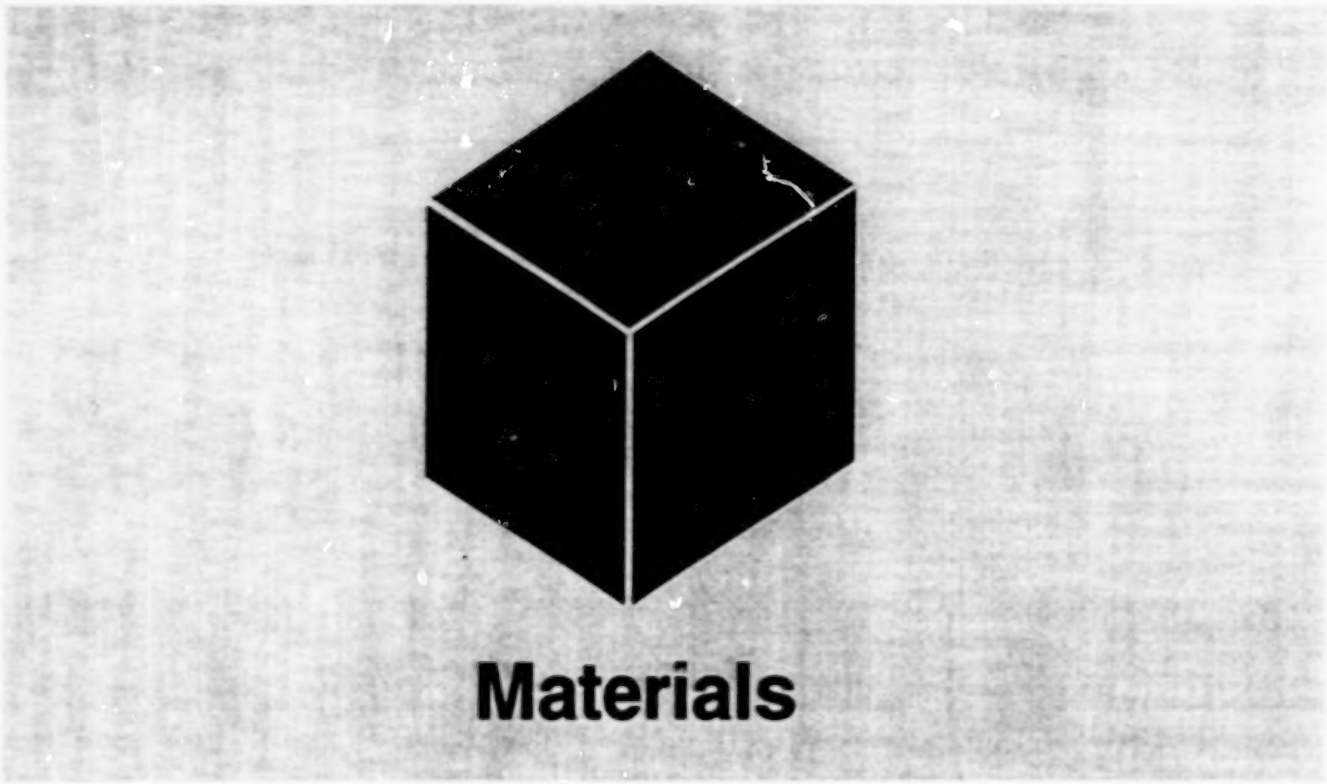

Materials

Hardware, Techniques, and Processes

25 CVD of Diamond Using Magnetoplasmadynamic Sources
26 Oxygen Batteries Based on a Solid Polymer Electrolyte

24

BLANK PAGE

CVD of Diamond Using Magnetoplasmadynamic Sources

Rates of deposition are expected to exceed those from other sources.

NASA's Jet Propulsion Laboratory, Pasadena, California

A program of research and development is addressing the feasibility of using magnetoplasmadynamic (MPD) sources in the chemical vapor deposition (CVD) of synthetic diamond films. Because of its unique combination of thermal, electronic, mechanical, and chemical properties, diamond has potential for use as a coating material in numerous engineering and scientific applications.

A large amount of research has been directed toward understanding and developing CVD process (including plasma-assisted CVD process) for the synthesis of diamond and diamondlike materials. The plasma-assisted CVD processes include some that involve dc-arcjet sources; the development of these processes has benefitted from extensive prior research on dc-arcjet thrusters for spacecraft. Rates of deposition that have been achieved by use of dc-arcjet sources have exceeded those achieved by use of other gas-activation sources.

The success of the dc-arcjet approach has led to speculation on the utility of other thruster-type plasma sources for CVD of diamond. There is a large body of data from previous research on the performance and plume characteristics of electric propulsion devices; these data are available to support continuing efforts to understand the reaction kinetics and growth chemistry of diamond. One logical extension of the prior research would be an assessment of electric thrusters, other than dc-arcjet thrusters, for their potential to increase rates of deposition even further. MPD thrusters are among those that could be considered.

Regarded as thrusters, MPD sources have been found to perform with low efficiency at power levels below a hundred kilowatts. However, some characteristics of the discharges and plumes from MPD sources indicate that these sources might be well suited to synthesis and deposition of diamond at rates higher and over areas larger than those achievable by use of dc-arcjet sources; the characteristics of particular relevance in this regard are higher levels of dissociation and ionization of gas in the cores of the plasma plumes, higher jet velocities, and the scaleability to higher power levels.

The experimental part of this research is being performed in a segmented stainless-steel vacuum chamber (see Figure 1). An argon-hydrogen discharge operating at a power level in the range of 10 to 20 kW is being used to demonstrate feasibility and explore the effects of substrate biasing. Methane serves as a carbon precursor for deposition of diamond and is injected just downstream of the anode plane through a molybdenum tube. Farther downstream, a water-cooled copper mount supports a removable molybdenum disk that serves as a substrate for deposition of diamond (see Figure 2). Windows would provide access for optical diagnosis at several locations. A monochromator will be used for all emission spectroscopy in the plume, and an optical pyrometer and thermocou-

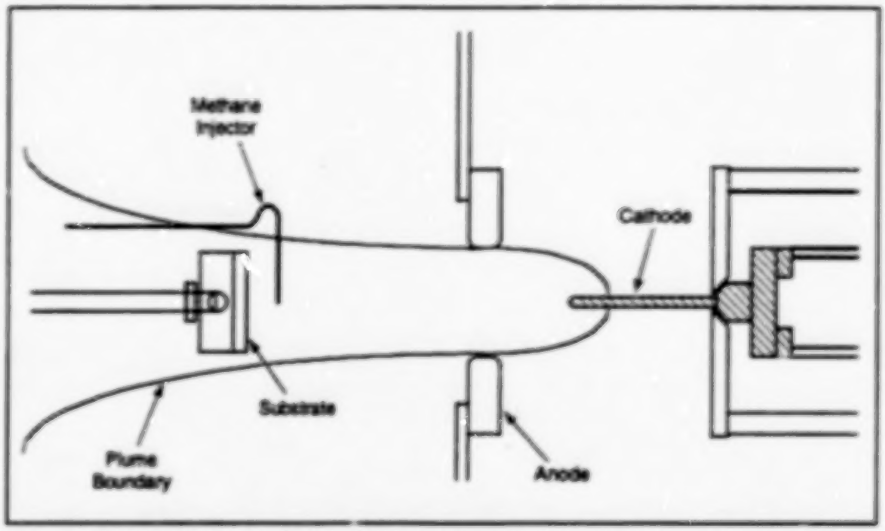

Figure 1. The Cathode Test Facility at NASA's Jet Propulsion Laboratory includes a vacuum chamber and associated equipment previously used to investigate the behavior of high-current, thermionic cathodes for high-powered electromagnetic thrusters. This schematic shows the arrangement of substrate and methane injector to the accelerator electrodes.

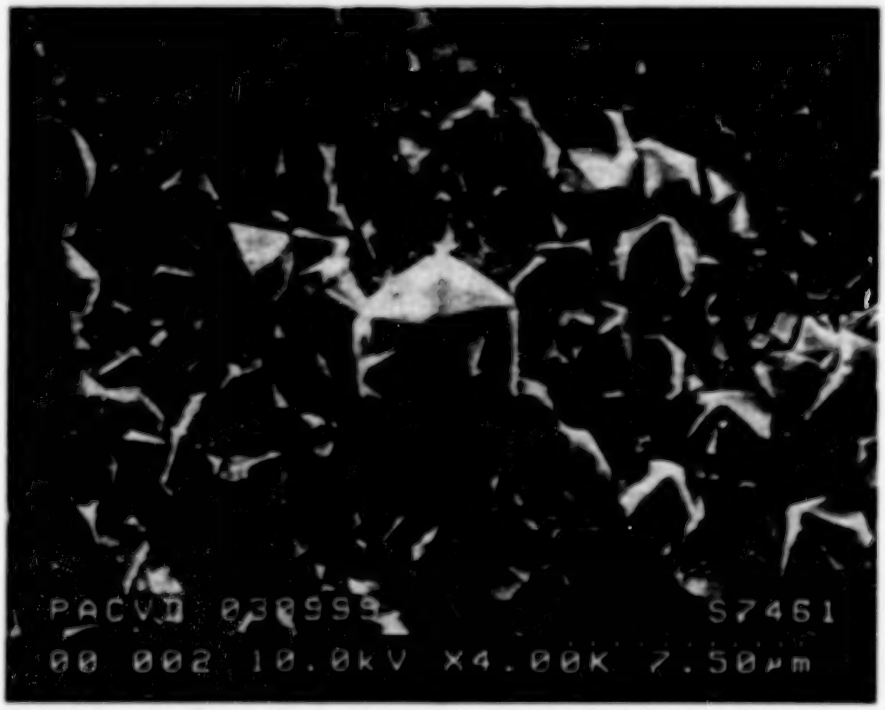

Figure 2. Scanning Electron Microscope Image (magnification 4,000×) of diamond film is shown (approximately 2.5 µm thick) grown over 180-minute test at low power (<20 kW) using a mixture of 1.5 percent methane to hydrogen by volume.

ples are used to measure the temperature of the substrate.

The research includes a combination of experimental and computational analyses of the MPD-assisted CVD process, designed to assess the feasibility of the process and to compare it with dc-arcjet-assisted CVD processes. Topics would include the following:

- Parametric sensitivity (effects of discharge power, gas mixture, substrate biasing, and background pressure on substrate temperature, film quality, area of deposition, and rate of deposition);
- Properties of the plasma plume (e.g., mean gas velocity, pressure, and temperature);
- The degree of pyrolysis of methane (assessed by means of spectroscopy of visible emission lines of C, H, and CH), in comparison with corresponding published information for arcjets;
- Gas-phase and surface chemistry (modeled computationally with the help of experimental and published data).

This work was done by James Polk, John Blandino, and David Goodwin of Caltech for **NASA's Jet Propulsion Laboratory**. *Further information is contained in a TSP [see page 1].*

In accordance with Public Law 96-517, the contractor has elected to retain title to this invention. Inquiries concerning rights for its commercial use should be addressed to

Technology Reporting Office
JPL
Mail Stop 122-116
4800 Oak Grove Drive
Pasadena, CA 91109
(818) 354-2240

Refer to NPO-20668, volume and number of this NASA Tech Briefs issue, and the page number.

Oxygen Batteries Based on a Solid Polymer Electrolyte

Oxygen gas is used as the electroactive cathode material.

Lyndon B. Johnson Space Center, Houston, Texas

Scientists have developed a derivative of the lithium-ion cell that could prove useful in space-flight and commercial applications in which it is planned to use oxygen batteries based on solid polymer electrolytes. This derivative cell, which contains a solid polymer electrolyte and an oxygen gas cathode, is designed for and operates best in an oxygen-rich atmosphere. (Inasmuch as the derivative cell as designed cannot store oxygen, the gas must be obtained from the environment.) Because the demand for portable electronic devices for scientific, educational, and even entertainment uses is constantly increasing, the need for rechargeable batteries as alternative means to power these devices is also increasing. Batteries based on the present derivative cell could be one such alternative means.

A unique feature of the polymer-electrolyte-based lithium cell is the way in which it utilizes (1) oxygen as an electroactive cathode (positive electrode) and (2) lithium — or another electroactive metal (e.g., magnesium, sodium, calcium, aluminum, or zinc) — as an anode (negative electrode). To implement this utilization scheme, the scientists sandwiched a lithium-ion-conductive solid polymer electrolyte film between a lithium anode and a composite carbon electrode that serves as the cathode current collector on which electroactive oxygen is reduced when the battery discharges to generate electric current. The simple design objective for these scientists was to devise a novel, solid-polymer-electrolyte-based lithium battery that could be used in spaceflight and industry.

The cathode current collector is, more specifically, made of a high-surface-area carbon (e.g., carbon black or graphite powder). In operation of the derivative cell, oxygen is reduced on the cathode collector. If lithium is the anode material, then the open-circuit potential of the cell is about 2.9 V, while the potential under load ranges between 2 and 2.9 V, depending on the load current. The theoretical specific energy of the cell is 5,200 Wh/kg — a value that makes the cell design useful, except in a vacuum, where it would be necessary to provide a self-contained supply of oxygen.

The design of the derivative cell can satisfy requirements of government and industry for rechargeable batteries that utilize oxygen gas cathodes. Because the design is experimental, anticipated cost savings cannot be surmised; however, the design holds promise and could provide another answer to the burgeoning need in the commercial marketplace and the U.S. space program for alternative forms of rechargeable batteries.

This work was done by Zhiping Jiang and Kuzhikalail Abraham of EIC Laboratories, Inc., for **Johnson Space Center**. *Further information is contained in a TSP [see page 1].*

In accordance with Public Law 96-517, the contractor has elected to retain title to this invention. Inquiries concerning rights for its commercial use should be addressed to

Zhiping Jiang
EIC Laboratories
111 Downey Street
Norwood, MA 02062

Refer to MSC-22790, volume and number of this NASA Tech Briefs issue, and the page number.

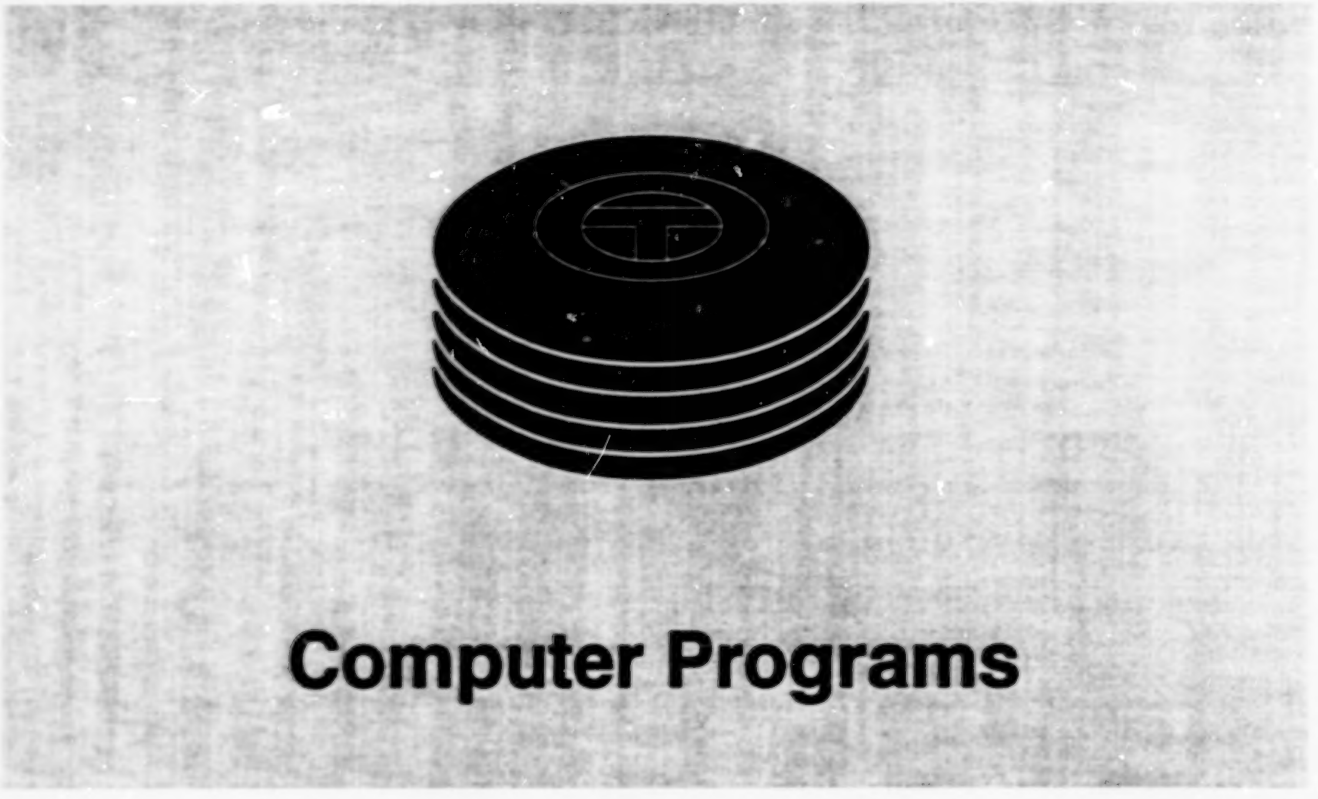

Computer Programs

Physical Sciences

29 Software for Analysis of Contamination of the ISS

BLANK PAGE

Physical Sciences

Software for Analysis of Contamination of the ISS

The NASAN computer program can perform detailed analyses of molecular column density and molecular deposition on and around such complex space structures as the International Space Station (ISS). Contamination from both point sources (e.g., thrusters and vents) and diffuse sources (e.g., reflected plumes or outgassing of materials) can be analyzed. NASAN is has been used to perform the assessments reported in the ISS incremental-design-review documents.

NASAN consists of several interactive tools (subroutines) that are linked together into a single, modular computer program that takes advantage of common program elements, which include manipulation of geometric models and plotting of results of computations. The central program components are designed to be easily expandable to perform additional analyses.

NASAN includes ray-tracing subroutines that are efficient means for calculating surface shadowing within the various program application modules. A variety of mathematical models of plumes can be easily called from the application modules. Two of these plume models calculate surface view factors, as needed, so that contamination calculations can proceed efficiently.

Because geometric models with as many as 25,000 surfaces can be analyzed, the fidelity achievable by use of NASAN is greater than that achievable with software developed previously for the same purpose. The modular structure of NASAN, along with a high degree of portability, makes it possible to perform contamination calculations on a much wider variety of computer platforms than was previously possible. Considerable time is saved over prior software of this type by use of NASPLT, which is a plotting subroutine within NASAN: this is because results of contamination calculations can be plotted from within the same subprograms that perform the calculations.

Another module of NASAN is CDPLT, which is a unique software tool for calculating and displaying the molecular column density around a spacecraft. This module has enabled the completion of numerous column-density calculations that, previously, could not be attempted.

Yet another module, FIRJET, models a surface plume and enables quick calculation of direct-flux molecular deposition onto a geometric model that has easily reorientable surfaces. The surface-source-plume model has enabled the analysis of more outgassing sources and model configurations than were previously possible.

The program is operational on several UNIX platforms, and some ray-tracing calculations can be performed in parallel on computers that include multiple processors. A simple, interactive user interface enables quick, interactive calculations, and facilitates setup for longer batch calculations. The contamination analyses performed by use of NASAN are helping to make possible the ISS design and verification activities to proceed on schedule. NASAN is also a powerful means for more detailed assessments of the local environments around specific payloads.

This program was written by Charles Lynn Hakes, Rose T. Rodriguez, Doug Warrington, and Eleazar Rios of Lockheed Martin for **Johnson Space Center**. *Further information is contained in a TSP* *[see page 1]*.

MSC-22963

BLANK PAGE

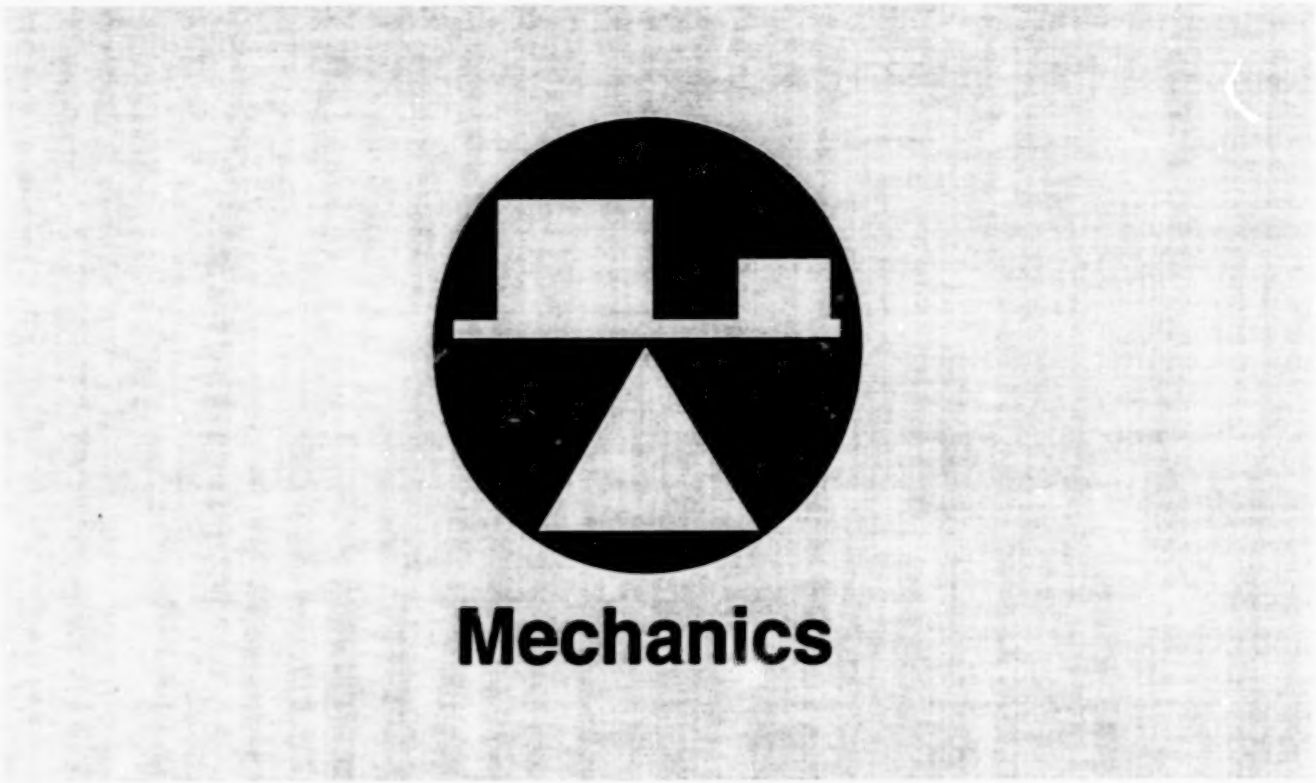

Hardware, Techniques, and Processes

33 Thrust Stand Measures Thrusts of <1 Pound

32

BLANK PAGE

Thrust Stand Measures Thrusts of <1 Pound

This device measures thrusts produced by miniature cold-gas thrusters in vacuum and air.

Lyndon B. Johnson Space Center, Houston, Texas

The development of miniature, cold-gas thrusters for on-orbit propulsion of such small devices as remotely piloted cameras and for inclusion in astronaut propulsion backpacks gave rise to a need to measure thrusts ranging from 0.04 to 0.8 lb (0.2 to 3.6 N). In addition, there was a need to measure thrust in a vacuum environment as well as in air at a pressure of 1 atmosphere (0.1 MPa), and over a wide range of propellant inlet pressures. The primary obstacle to be overcome for such measurements was to solve the problem of delivering the cold-gas propellant (compressed nitrogen gas) to the thruster without affecting thrust measurements, particularly those below 1/4 lb (1 N).

Methods for measuring larger thrusts include the use of flexible tubes or rotating fluid couplings to deliver propellants. However, in the present low-thrust application, the forces applied by flexible tubes to thrust sensors would be large with respect to the thrust being measured. In addition, the forces generated by flexible tubes vary with changes in propellant pressures and apply off-axis loads to the thrust sensors. The internal frictional forces in rotating fluid couplings, and the variations of these forces with pressure, would also be too great with respect to the low thrusts to be measured.

The figure is a cross section of a thrust stand designed for measuring small thrusts in vacuum or in air at atmospheric pressure. A readily available doughnut-configuration load cell is used as the thrust sensor. The doughnut configuration was chosen because its central hole makes it possible to make the propellant-flow path coaxial with both the thruster and the load cell. The load cell is equipped with a vent port so that the pressure of air in its internal cavity always equalizes with the pressure of the surrounding air, to prevent undue pressure-related shifts in load-cell output.

A flange assembly and flow stem are included to provide for delivery of propellant coaxially through the load cell to the thruster. The flow stem is also part of a thruster-mount fitting, which transfers thrust from the thruster to the load cell. The coaxial arrangement of the thruster, load cell, and flow stem eliminates all off-axis loads.

The flow stem was designed to protrude through both the top and bottom flanges so that propellant pressure is axially balanced on the stem in opposing directions. This was done to negate the force on the load cell produced by the static pressure and by variation of the static pressure of the propellant. In practice, this design feature proved successful, balancing 98.7 percent of the force [7.8 out of 7.9 lb (34.7 out of 35.1 N)] at a propellant pressure of 258 psi (1.78 MPa).

One focus of design efforts was the problem of how to best seal the gap between the flow stem and the flanges to prevent the escape of nitrogen, while allowing for consistent reactions from the load cell for a given thrust. Initially, the flange passageways incorporated internal O-ring grooves, with the O-ring sealing against the flow stem in the top and bottom flange. Since full deflection of the load cell was <0.001 in. (<0.025 mm), the seals could be regarded as parts of a static configuration in which the O rings served as flexures to a tiny extent. In practice, however, the O rings tended to shift in their grooves with variations in propellant pressure, thus yielding inconsistent readings from the load cell.

To provide an alternate method of sealing between the flow stem and flanges to eliminate shifting of the seals, O rings were replaced with a silicone sealant. It was reasoned that once the sealant became cured, the adhesion of the sealant to the flow stem and flanges would ensure a fixed geometry, without the slippage between dissimilar surfaces that had occurred in the use of the O rings. Like the O rings, the new silicone seals would flex microscopically, but they would not slip along the flow stem or shift in their grooves as the O rings did. A pourable silicone sealant with proper viscosity in the uncured state and proper shear strength in the cured state was selected. An assembly method and tools were devised to support pouring and curing of the silicone seals during assembly of the thrust stand. During testing of the silicone seals, no leakage was observed at pressures up to 270 psi (1.86 MPa).

Additional features of the thrust stand include the following:

- A shoulder on the thruster mount fitting holds preload weights that are needed to optimize the sensitivity of the load cell.
- A raised wall on the top flange protects

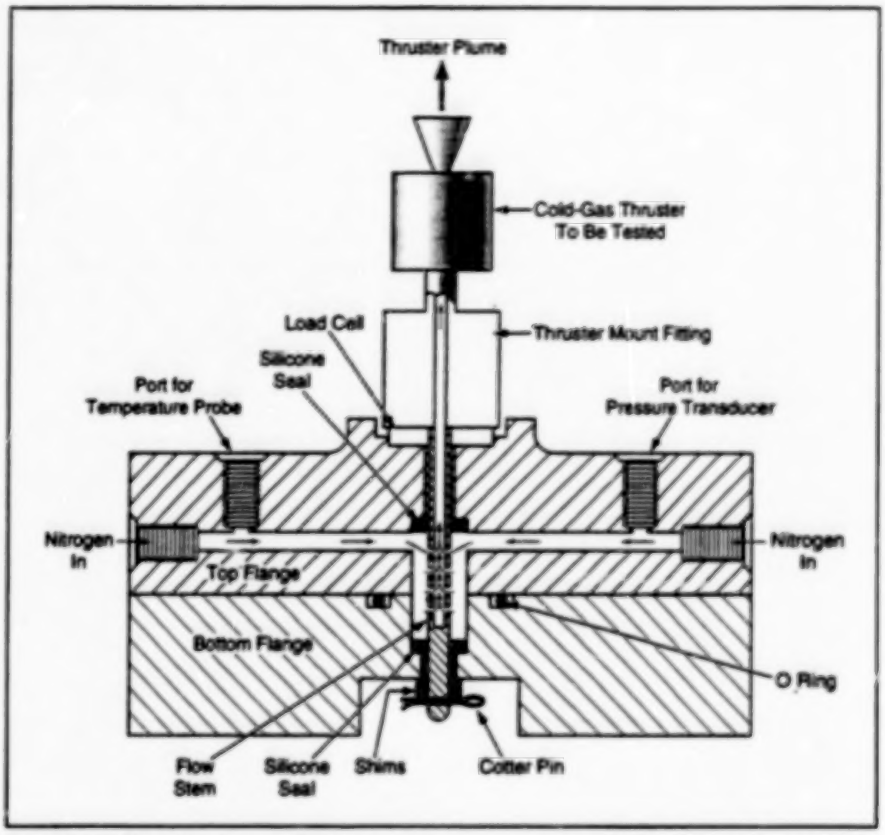

This Thrust Stand has been calibrated to yield accurate measurements of thrusts from 0.02 to 0.61 lb (0.09 to 2.7 N). This view is a simplified cross section; some details are omitted.

the load cell, which is delicate.

- Leakage relief paths from the silicone seals prevent unwanted pressurization in the event of a leak.
- Ports for temperature and pressure sensors are included.
- A cotter pin and shims retain the flow stem in the flange assembly. Shim stack height is set as needed to carry any inadvertent loads applied to the bottom of the flow stem during handling and installation, thus protecting the silicone seals from damage.

Calibration of the thrust stand began with pressurizing it to one of the pressures desired for testing thrusters. Next, calibrated brass weights were placed on the thruster nozzle, and the electrical output of the load cell was recorded. After calibrations were completed, the thruster was fired several times, then calibration was repeated.

During a test program, the thrust stand was calibrated in thrust ranges of 0.02 to 0.16 lb (0.09 to 0.71 N) and 0.39 to 0.61 lb (1.7 to 2.7 N). The error in the measurements was ±5 percent of indication in the low range and ±3 percent of indication in the higher range. This combination of ranges and accuracies amounts to an exceptionally wide useful overall range for a thrust-measurement system. The thrust measurements obtained in thruster firings were found to be equally or more repeatable (that is, characterized by error bands of equal or smaller width), in comparison with the thrust measurements obtained during calibration.

Further changes in the design of the thrust stand have been proposed to increase its capability for future use. Mounting the load cell under the bottom flange in a holding fixture would make it possible to replace the load cell easily with a load cell of a different measurement range. Thrust would still be transferred to the load cell coaxially, but it would be transferred from the bottom tip of the flow stem, through a thermal-isolation fitting, to the load cell. Not only would the replacement of the load cell be much simpler; in addition, this configuration would thermally isolate the load cell from the thruster and propellant, thus providing for temperature conditioning of the thruster and propellant beyond the range allowable for the load cell. This configuration would also make it possible to use a larger diameter flow stem to accommodate thrusters with higher flow rates.

In this application, time constraints dictated the purchase of a best available, off-the-shelf load cell that had a normal measurement range of up to 2 lb (8.9 N). The use of the load cell for a wide range of measurements is what made it necessary to perform both a low-range calibration and a separate high-range calibration to ensure accuracy. Time permitting, future versions of the thrust stand would incorporate lower-range load cells for the lowest of thrust measurements.

This work was done by Mark L. Villemarette of* **Johnson Space Center**. *Further information is contained in a TSP [see page 1].*

MSC-22861

*Presently of Oceaneering Space Systems.

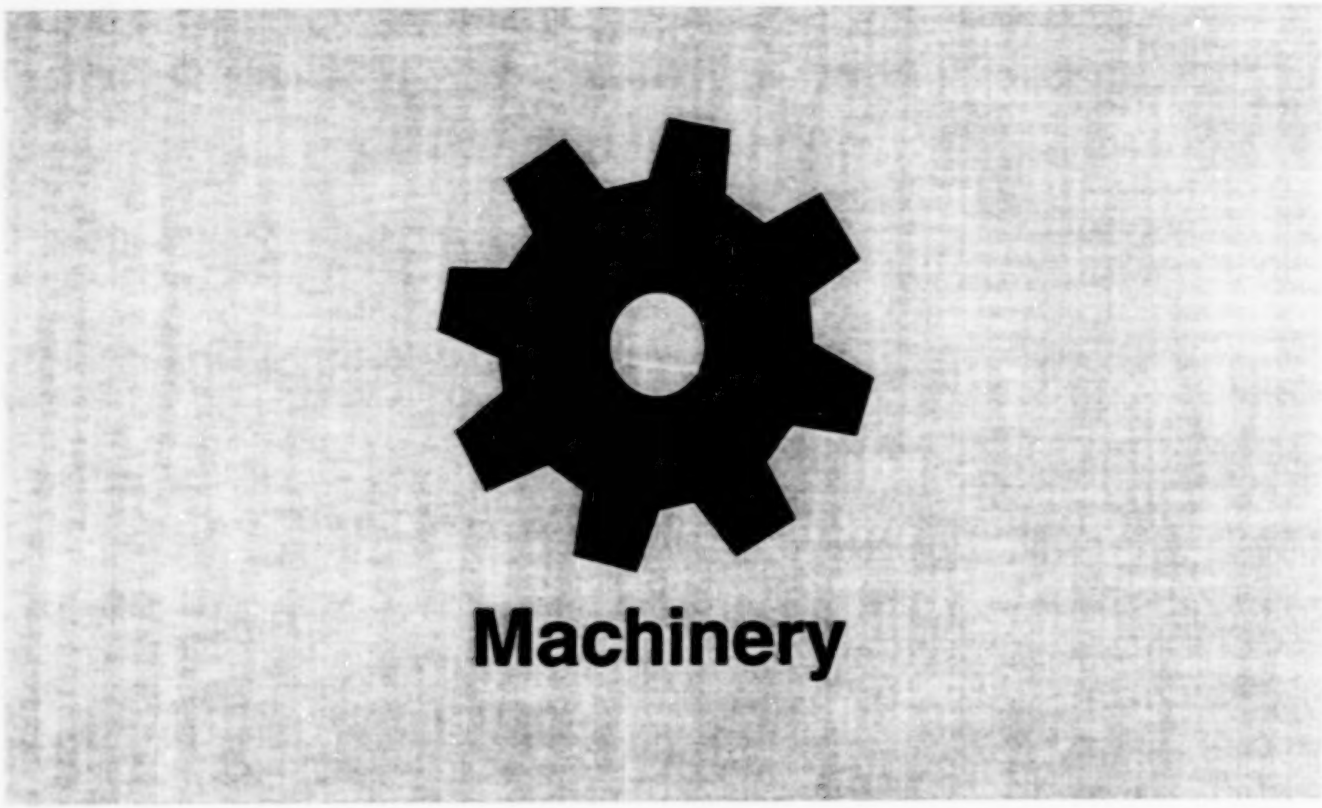

Machinery

Hardware, Techniques, and Processes

37 Moving Chair for Virtual Reality

BLANK PAGE

Moving Chair for Virtual Reality

The chair provides a combination of synthetic motion and support in a minimally stressful posture.

Lyndon B. Johnson Space Center, Houston, Texas

An apparatus called a "personal motion platform" (PMP) is undergoing development for use in adding the sensations of motion to computer-controlled simulated environments of the type now popularly known as virtual reality. The PMP was conceived originally for training an astronaut to interact with surrounding objects in a simulated zero-gravitation environment; it also has obvious potential for use in a variety of applications in biomedical research, education, and entertainment.

The PMP (see figure) includes a chair that supports the occupant in a modified version of the neutral body posture of zero gravitation. The chair is supported by a three-degree-of-freedom system of linear electric-motor actuators. A computer commands the actuators to produce the desired synthetic motions, which are reminiscent of computer-controlled motions of aircraft cockpit flight simulators. The PMP is also equipped with hand-operated controls.

The motion commands for actuators are computed partly from a combination of (1) a mathematical model of the synthetic environment, (2) the kinematics of the chair, and (3) position feedback. In addition, to enhance the interaction between the user and the synthetic environment, motion commands can be derived from simulated collisions with objects and from the hand-operated controls. As in the case of flight simulators, the computed motions are adaptively filtered to retain as much as possible of acceleration frequency components needed for realistic sensations of motion while limiting overall excursions to avoid hard stops at the limits of the actuators.

The Reclining Chair Pitches, Rolls, and Heaves as it holds the occupant in a minimal-stress posture intermediate between the neutral body posture of zero gravitation and a normal posture of relaxation on a flat, level surface. Linear electric motors at the base of the chair drive the motion.

This work was done by Brian Park of Flogiston Corp. for **Johnson Space Center**. *Further information is contained in a TSP [see page 1].*
MSC-22623

BLANK PAGE

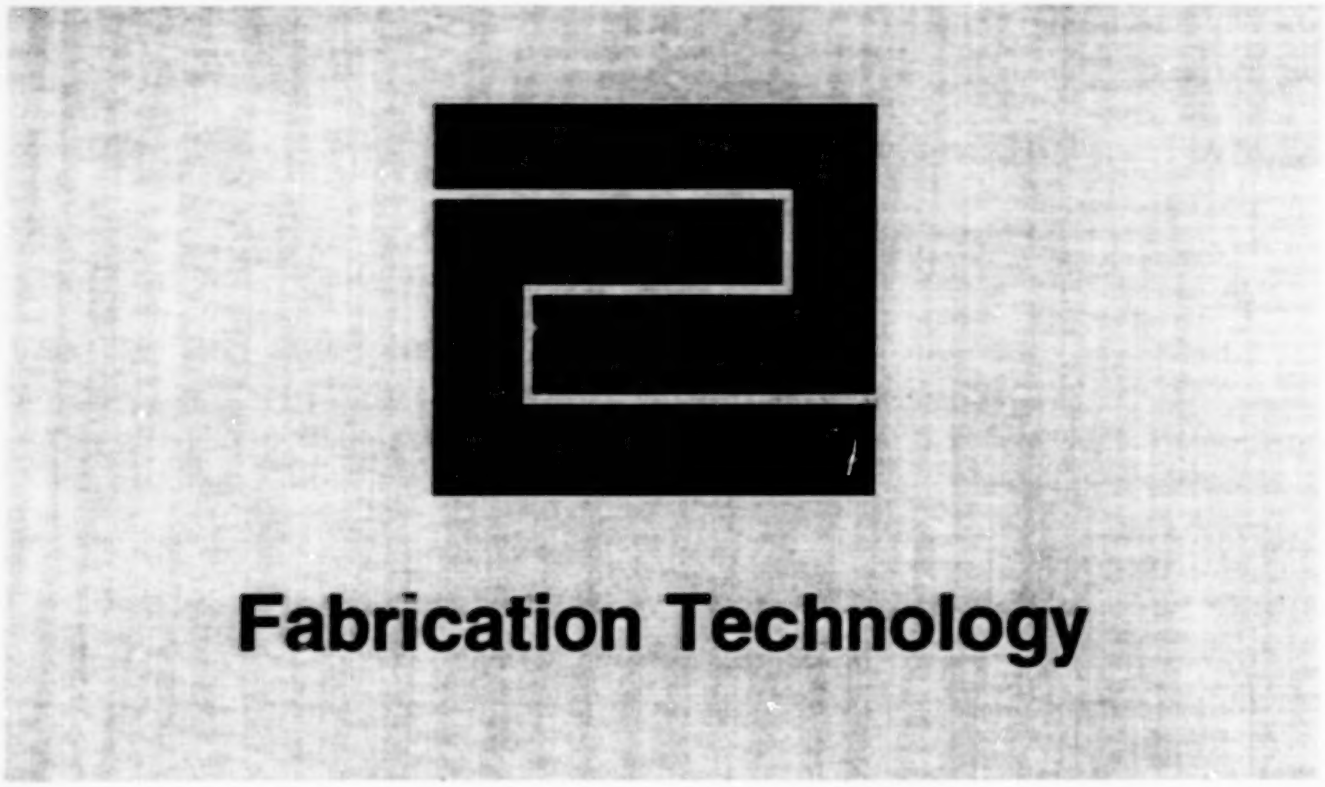

Fabrication Technology

Hardware, Techniques, and Processes

41 Gap Welding Preforms

BLANK PAGE

Gap Welding Preforms

Ribbon RF connections could be made with greater consistency.

Goddard Space Flight Center, Greenbelt, Maryland

Small, temporary, disposable inserts, called "gap welding preforms," have been proposed for use in attaching electrically conductive ribbons to radio-frequency (RF) electronic circuits. As explained below, the use of gap welding preforms would help to ensure consistency of the ribbon connections and would reduce the time necessary for making the connections.

In the situation that inspired the proposal, gold ribbons 0.025 in. (0.64 mm) wide and 0.001 in. (0.025 mm) thick must be formed and attached to RF circuitry under a microscope up to 0.6 in. (15 mm) deep into RF housings. A ribbon must be manually held in place and formed to the required strain-relief arch between connection points by use of tweezers and other small tools, according to the best judgement of a technician. The ribbon is attached by use of a gap welding machine that includes small probes for placing welds. The technician's view of the ribbon through the microscope can be limited, especially inasmuch as side viewing is usually not possible. Sometimes, this difficult forming-and-attachment procedure inadvertently results in excessive strain-relief arch, which can degrade the RF signal and thus make it necessary to rework the connection.

A gap welding preform would be made of a material that could hold a predetermined shape and could be easily removed after use without causing any deterioration of the welded ribbon or the surrounding material. For example, a gap welding preform could be made of a thickened acrylic compound similar to that used for conformal coating of circuit boards. Thickeners and solidifiers could be mixed into the material to facilitate extrusion into various predetermined shapes. A gap welding preform for a given application would be shaped so that a ribbon laid on it during a forming-and-attachment procedure would end up shaped in the strain-relief arch required for that application.

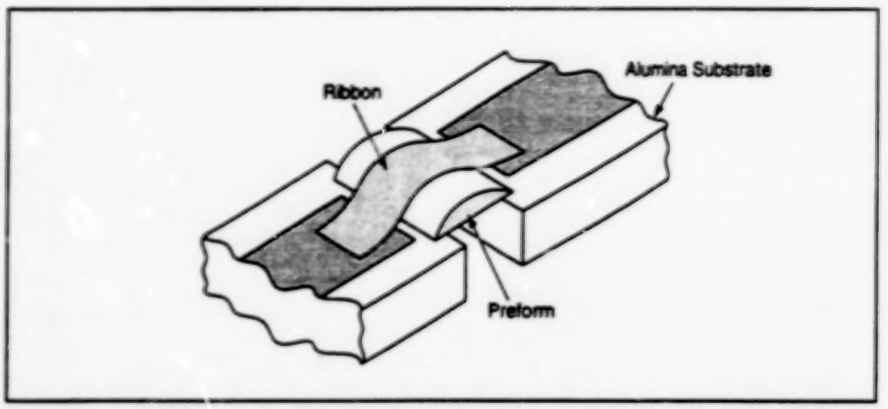

The Preform Is Placed in the Gap between contact points to which the ends of the ribbon are to be welded. The ribbon is shaped to the desired strain-relief arch by bending it on the preform.

The steps in the use of a gap welding preform would be the following:

1. The preform would be cut to a length greater than the width of the ribbon to be attached.
2. The preform would be placed between the connection points in the circuit path.
3. The ribbon would be formed over the preform (see figure) and one end of the ribbon would be welded in place.
4. The ribbon would be examined to determine whether it was in the desired shape and, if not, would be reformed as necessary.
5. The ribbon would be welded in place at the end not previously welded.
6. The preform would be dissolved by a suitable solvent (e.g., alcohol) and the ribbon connection would be inspected. The use of dissolution (instead of another method) to remove the preform would eliminate the risk of tearing the welded ribbon, reduce the time needed to remove the preform, and reduce the time needed for inspection.

This work was done by Richard F. Davis and Mark A. Hillyer of Hughes Electronics Corp. for **Goddard Space Flight Center.**
GSC-14103

42

BLANK PAGE

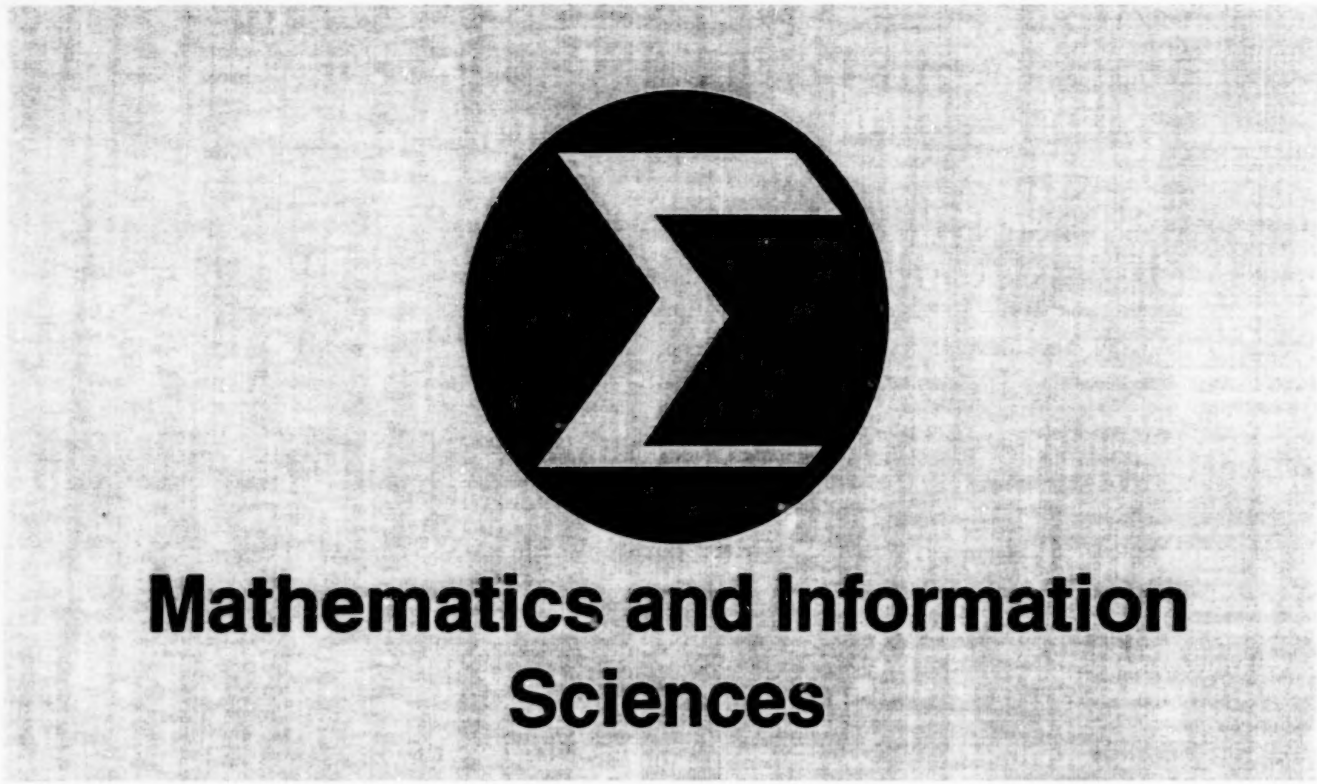

Mathematics and Information Sciences

Hardware, Techniques, and Processes

45 Knowledge-Based Software for Generating and Changing Plans
46 Numerical Speed of Sound
46 Software To Detect Malfunctions in Anesthesia Equipment
47 Program for Viewing Remotely Generated Summary Data
47 Electronic Time-Card System

BLANK PAGE

Knowledge-Based Software for Generating and Changing Plans

Effects of changes in requirements and resources are automatically taken into account.

Lyndon B. Johnson Space Center, Houston, Texas

A methodology of computer-aided planning has been developed to (1) accelerate the generation of plans for activities within complex systems of personnel and equipment; (2) increase the quality of the plans thus generated; and (3) decrease the difficulty of predicting and responding to the effects of changes in plans, requirements, resources, and/or other constraints. Originally intended for application to planning of missions of the space shuttle and other spacecraft, the methodology could also be applied to strategic business planning, management of projects, general scheduling, and planning of manufacturing processes and systems.

The three principal components of the methodology are (1) an ontology of mission planning; (2) knowledge-based algorithms and conceptual (including mathematical) models for the analysis of plans; and (3) the Knowledge Aided Mission Planning System (KAMPS) computer program, which embodies the ontology, algorithms, and models. The KAMPS software implements a structured method for planning and replanning. The KAMPS planning method involves (1) a template-based approach to the generation of plans; (2) representation, from alternate perspectives, of knowledge about plans, application of plans, and maintenance of plans; and (3) qualitative and quantitative analysis of plans for prediction of the effects of changes.

The ontology and an associated theoretical framework were developed to enable detailed characterization of the world for the purpose of performing mission planning in this domain. The ontology and framework provide a conceptual foundation for knowledge-based creation, maintenance, and analysis of plans. The development of the ontology included the characterization of the key entities involved in the mission-planning process, and of the relationships and constraints that govern the behavior of those entities. This development effort resulted in a characterization of the ontology and the production of information models and process models for the mission-planning domain.

KAMPS provides means for capturing the information that pertains to the flight-design process, reasoning with this information to assist in developing plans, and to assist in the analysis of the effects of plans and of changes. KAMPS is based on a very clear and succinct modeling paradigm in which all of the information is managed in three views: product-centered, activity centered, and resource-centered. The concepts that occur in each of these views and the relationships among the various concepts were studied and are implemented in KAMPS. The use of KAMPS for the flight-design process is expected to encourage the user to perform modeling and design according to the best practice and research conventions, which have been incorporated into KAMPS.

KAMPS incorporates a rich library of qualitative and quantitative conceptual models for predicting the effects of changes. Temporal effects are included in quantitative predictions; effects on values, processes, inputs, and outputs are included in qualitative predictions.

KAMPS facilitates modeling of products and activities at multiple levels of abstraction. KAMPS also supports planning and reasoning at multiple levels: For example, upper managers can use KAMPS to do planning at a relatively abstract level, whereas middle managers can use KAMPS to perform planning at a more detailed level.

Once experience with KAMPS results in the accumulation of sufficient pertinent information about flights and templates, it should be possible to use KAMPS as means to provide detailed information on the flight-design process that is detailed, standardized and more complete than the information in the flight-design handbook used heretofore for training. In comparison with the handbook, KAMPS presents relevant information in ways that are more interactive, modular, and graphical. Thus, KAMPS can serve as both a means to document the NASA flight-design process and as a tool for training.

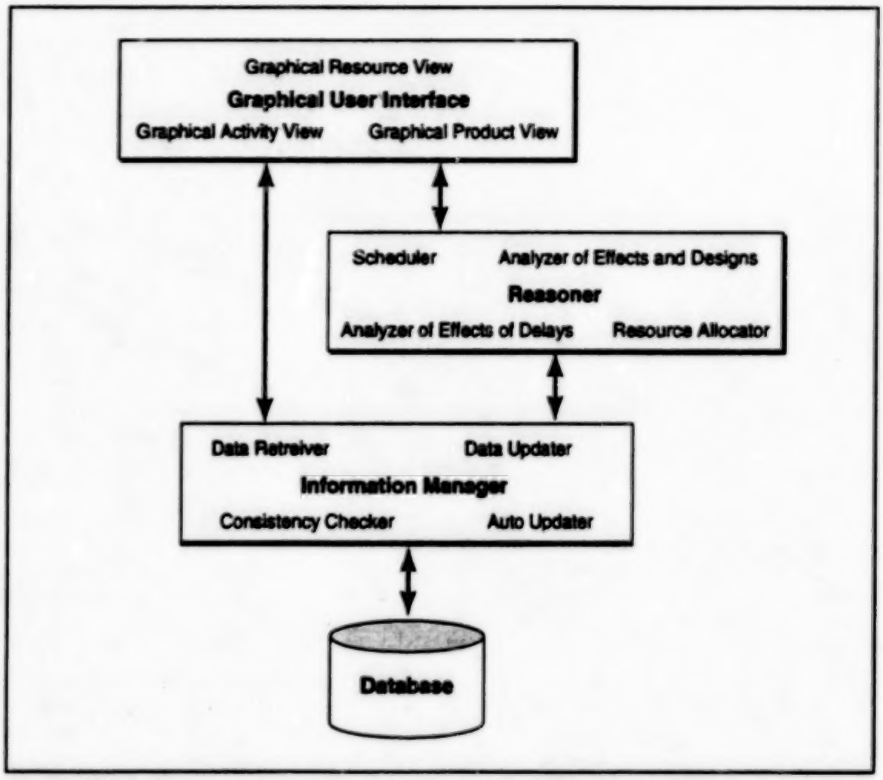

The KAMPS Software is divided into four modules, each of which performs a different set of functions.

This work was done by Benjamin Perakath and Blinn Thomas of Knowledge Based Systems, Inc., for **Johnson Space Center.**

MSC-22830

Numerical Speed of Sound

This concept is applicable to flows at all speeds.

John H. Glenn Research Center, Cleveland, Ohio

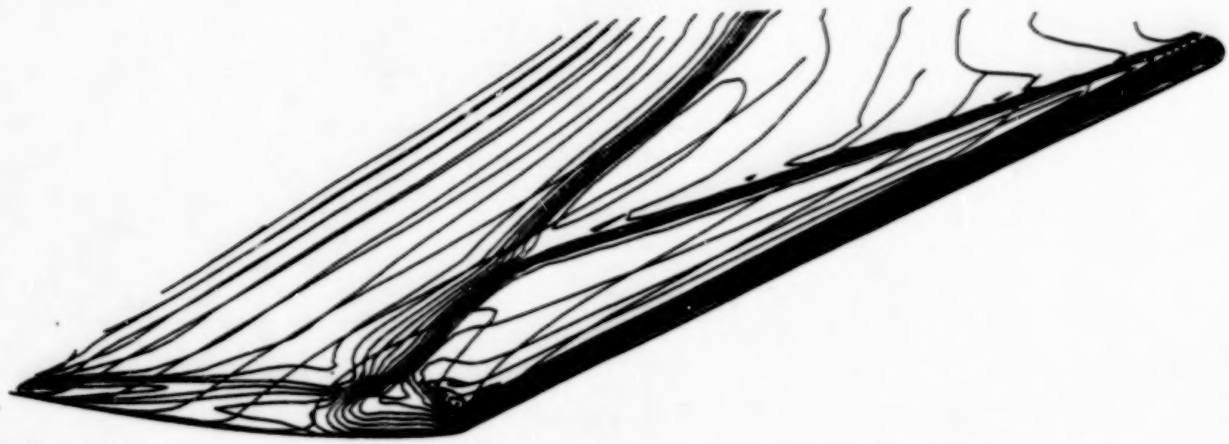

Pressure Contours on a Wing were computed by using a scheme called "AUSM+," augmented with the numerical speed of sound, to solve the Navier-Stokes equations numerically. The wing is of the M6 type of the Office National d'Etudes et de Recherches Aérospatiales (ONERA). The flow conditions for this computation were a free-stream speed of mach 0.84, a Reynolds number of 18.2×10^6, and an angle of attack of 3°. The computed pressure contours are in good agreement with available experimental data, especially in capturing two shocks that manifest themselves in the λ-shaped pattern of closely spaced curves.

The numerical speed of sound is a variable that is used in the numerical solution of flows from low to high speeds. The numerical speed of sound is an effective speed of sound associated with Mach numbers used in the numerical splitting of a flow into upwind and downwind mass-flux components that are defined on the faces of cells of a computational grid into which a flow volume is divided. Depending on the details of a given flow problem and the algorithm chosen to solve it, the numerical speed of sound may or may not equal the physical speed of sound.

The numerical speed of sound has been found to be very useful in constructing upwind numerical-solution schemes to satisfy certain criteria. [As used in this special context, "upwind" (as distinguished from "central" or "downwind") refers to a manner of approximating spatial derivatives of flow quantities by taking differences between discretized flow quantities at locations biased toward the upwind side with respect the location of immediate interest.] An especially notable criterion is the capability for exact capturing of contact and shock discontinuities in one-dimensional flows. The concept of the numerical speed of sound can also be extended to apply to the computation of low-speed (in effect, incompressible) flows. In such an application, a scaling factor that varies with speed is introduced. As a result, the numerical dissipation decreases with the flow speed and, as a further consequence, the rate of convergence of iterative computations toward the solution is increased. The accuracy of the solution is also increased.

In a study, the numerical speed of sound was incorporated into some numerical-solution schemes based on a method called advection-upstream-splitting method (AUSM). It can also be incorporated in other upwind schemes, including one known as Roe flux splitting, wherein an averaged speed of sound, among several other averaged variables, is automatically required. Other numerical-solution schemes can also be made to capture shocks exactly.

This work was done by Meng-Sing Liou of **Glenn Research Center** *and Jack R. Edwards of North Carolina State University. Further information is contained in a TSP [see page 1].*

Inquiries concerning rights for the commercial use of this invention should be addressed to NASA Glenn Research Center, Commercial Technology Office, Attn: Steve Fedor, Mail Stop 4–8, 21000 Brookpark Road, Cleveland, Ohio 44135. Refer to LEW-17011.

Software To Detect Malfunctions in Anesthesia Equipment

Response times in critical situations can be reduced.

Lyndon B. Johnson Space Center, Houston, Texas

To reduce response times and save lives in operating rooms, community trauma centers, and remote combat care facilities, a team of scientists working on behalf of Lyndon B. Johnson Space Center (JSC) has developed an artificial-intelligence alarm-management software system that detects malfunctions in esophageal intubation and anesthesia machines. This system uses CLIPS [the C-Language Integrated Production System] knowledge-based rules derived from real-time data supplied by a sheep model. Although this system is one of several current alarm-management software systems, it is vastly superior to the commercial software systems designed to perform the same or similar functions.

Commercial software systems of this type monitor faults that occur above or below preset thresholds. Threshold settings may vary, but the monitors are unable to detect faults "intelligently." They are, in effect, hampered by preset values and can

mistake threshold issues for life-endangering malfunctions. Because of this possibility of error, an alarm must always be treated as a serious matter, whether or not there is a malfunction. In an operating room, when an alarm warns of a possible malfunction, the surgical procedure can be disrupted. Without intelligent software already in place, surgical team members must verify that a malfunction has indeed occurred, or will occur, thus increasing both their own response time and the risk to the patient. A change is needed.

An artificial-intelligence software system that can detect and define faults accurately while it monitors patients on esophageal intubation and anesthesia machines would decrease response times and reduce risks to patients. CLIPS, the artificial-intelligence software designed at JSC, is a decision-support tool that can effect this change because CLIPS can be taught to determine the parameters of machines.

Basically, an artificial neural network implemented in software in a computer mimics the thought processes of the human brain. CLIPS follows pathways of reasoning, very like human thought processes, to eliminate possibilities. To support CLIPS, data are needed to design a program unique to the esophageal-intubation and anesthesia-machine environment; it is from these data that intelligent software can learn. The task for the team of scientists was to gather these data. For them, gathering data was an integral part of the development of the needed artificial-intelligence software system. The scientists selected a sheep model from which to elicit real-time data; from this model, the team compiled clinical annotations to validate their software system — all without risk to human patients.

Other artificially intelligent systems fail to provide similar annotations. For example, one prototype simulator that enables users to control and monitor an anesthesia delivery system resembles the JSC software. However, because all of its data and faults are simulated, it lacks the validation of real-time data. In short, no animal-model testing was done for this prototype. Thus, the major limitation of this and other currently available systems is the impossibility of validating them in environments in which they can be used without interfering with normal routines or endangering patients. Yet the user-interface design is critical, and artificial-intelligence software can learn from the results of animal model testing.

During the team effort, advances in artificial-intelligence software were applied to develop an expert system that could provide, to medical personnel, decision support on the condition of the patient and the anesthesia machine. The rules of the knowledge-based domain were defined by data extracted from various sources, including supporting literature, medical experts, and the sheep model. The prototype software that emerged from this process is still in an early stage of development; it will be tested further by users in a laboratory. The data generated by the sheep model will be analyzed and, if the analysis warrants, the design of the user interface will be modified. The inventors believe that more data should be collected, and hope to test 20 to 30 additional sheep to refine the quality of the expert-system rules being written. This would enable the validation of the software in real time to determine sensitivity and specificity in recognizing alarm conditions.

CLIPS-based software can detect malfunctions in esophageal intubation and anesthesia machines because the software uses the sheep model to provide real-time data from which knowledge-based rules are built. Because the reported malfunctions will be genuine, this system will reduce response times. The use of the real-time data from the sheep model sets this software system apart from other, commercially available artificial-intelligence software systems of this type. Once the sheep model has been fully demonstrated, the scientists anticipate that the system will be tested on human patients — in a way that does not interfere with patient care and adheres to standard medical practices.

This work was done by Todd T. Schlegel of **Johnson Space Center** *and Karin C. Loftin of KRUG Life Sciences, Inc.; Travis A. Moebes of Science Applications International; Jurine Acloff of Lockheed Martin; Donald J. Deyo of the University of Texas Medical Branch; and Jeffrey M. Feldman of the Albert Einstein Medical Center.*
MSC-22675

Program for Viewing Remotely Generated Summary Data

The Beacon Visualization (BeaVis) computer program provides a ground-based computing environment for displaying, tracking, storing, and maneuvering through telemetric data streams that contain summaries of engineering data generated aboard a spacecraft. BeaVis can also serve as a general-purpose software tool for monitoring data of other specific types. In the original spacecraft-to-ground application, BeaVis enables the user to scroll through a graphical depiction of telemetry downlinks to select desired data. Summary data are represented graphically, with hypertext links to strip charts of sensor channels represented by summary data packets. BeaVis also generates time-line and tabular displays. A time line depicts when, during a spacecraft mission, summary downlinks and beacon tone detections have occurred. The tabular and strip-chart displays are available through hypertext links from the time-line display. BeaVis also provides graphical user interface elements that show such specific summary data components as changes in mission activities, snapshot telemetry, episode data, and user summary data. The program also includes a software tool for creating tables of parameters that are uploaded to a spacecraft.

This work was done by E. J. Wyatt, Robert Sherwood, and Tim Fogarty of Caltech for **NASA's Jet Propulsion Laboratory**. *Further information is contained in a TSP [see page 1].*

This software is available for commercial licensing. Please contact Don Hart of the California Institute of Technology at (818) 393-3425. Refer to NPO-20665.

Electronic Time-Card System

A computer-based automated system has been developed to replace a cumbersome and error-prone paper-based system for recording employees' work times. The automated system minimizes the consumption of paper and eliminates the need for weekly pick-up and delivery of time sheets throughout the Kennedy Space Center. The computer-based system simplifies daily entry of times by employees, who select jobs worked from lists provided by supervisors. Employees "sign" their "time cards" electronically at the end of each week. Supervisors can review employees' electronic time cards daily and

can sign the time cards of employees under their supervision at the end of each week, all electronically. The system accommodates reassignment of employees to different departments or supervisors, as well as replacement of supervisors who call in sick. The system software automatically enforces rules that control the processing of time-sheet, payroll, and project data, including rules on who can charge how much time to which account. The electronic-time-card system was compiled using Visual Basic incorporating SQL server.

This work was done by James W. Thorpe, James P. Williams, Larry D. Jewell, Doris L. Bailey, Debra S. Blum, and Shirley R. Curry formerly of EG&G Florida, Inc., for **Kennedy Space Center**.

Inquiries concerning rights for the commercial use of this invention should be addressed to Lew Parish, Technology Counselor, Kennedy Space Center, (321) 867-6373. Refer to KSC-12051.

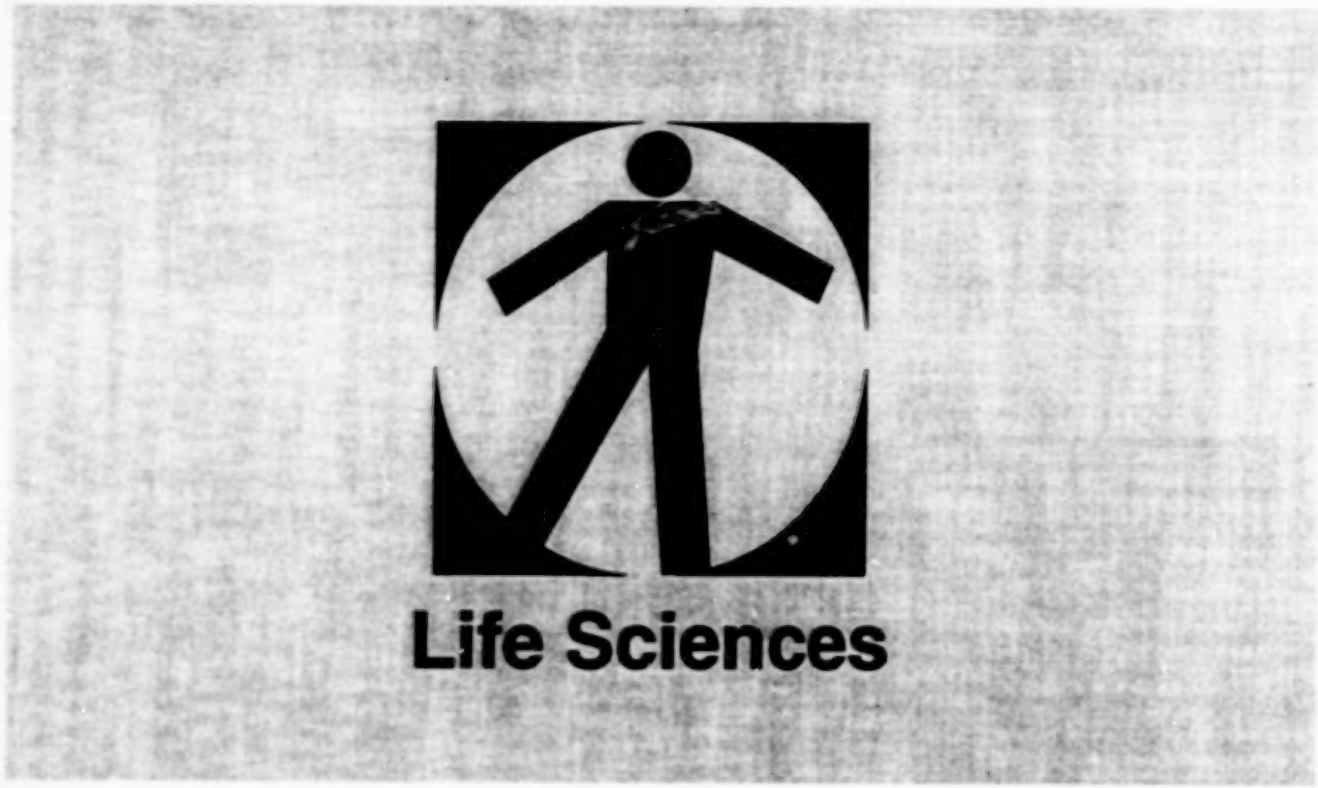

Life Sciences

Hardware, Techniques, and Processes

51 Apparatus Measures Attachment or Detachment of Biofilm
52 Device for Testing Susceptibility of Bacteria to Antibiotics
53 Improved Unidirectional Cell-Stretching Device

BLANK PAGE

Apparatus Measures Attachment or Detachment of Biofilm

Efficacy of a biocide can be assessed quantitatively.

Lyndon B. Johnson Space Center, Houston, Texas

Figure 1 schematically illustrates a laboratory apparatus that provides quantitative information on the density and on the rate of increase (or decrease) of density at which bacteria attach themselves to solid surfaces in a potable-water-supply system. These biofilms are potentially pathogenic and/or phytotoxic and can adversely affect processing of the water under some circumstances. The apparatus was devised to assess the abilities of biocide chemicals in water to suppress the biofilms in potable-water subsystems within closed life-support systems of spacecraft, but may also be adaptable to similar investigations of biofilms in terrestrial water supplies.

The apparatus implements a recently developed method of automated image analysis for continuous, real-time monitoring of attachment of microbes to (or detachment of microbes from) a surface of interest that is immersed in water containing the microbes and chemical(s) to be investigated. The surface of interest is located in a flow-chamber/optical-cell (FOC), which is a modified fungal-growth chamber with interior dimensions of 30 by 5 by 2 mm. Monitoring is performed by use of a video camera mounted on a microscope that is focussed on the surface of interest.

Water is recirculated through the FOC at a rate of 9.8 mL/min by a high-speed micropump. The pump produces a pulsating flow; the pulses are damped by a device of 1-mL volume upstream of the FOC. The influent and effluent tubes are positioned to achieve turbulent flow in the middle of the FOC, where the monitored surface is located.

The video images of the monitored surface are preprocessed into binary images. Then a frame grabber grabs two successive images and stores an average of them on an optical disk. The averaged image is processed to extract information on the number and total area of objects (attached bacteria) in the field of view. This process can be repeated at intervals, yielding cell counts that can be plotted as a function of time, to determine rates of attachment and/or detachment.

In a typical experiment, water containing a suspension of microbes is first circulated through the FOC for 18 to 24 hours, during which time some microbes attach themselves. Images are analyzed during this time to acquire data on the rate and density of attachment. Then the FOC and its

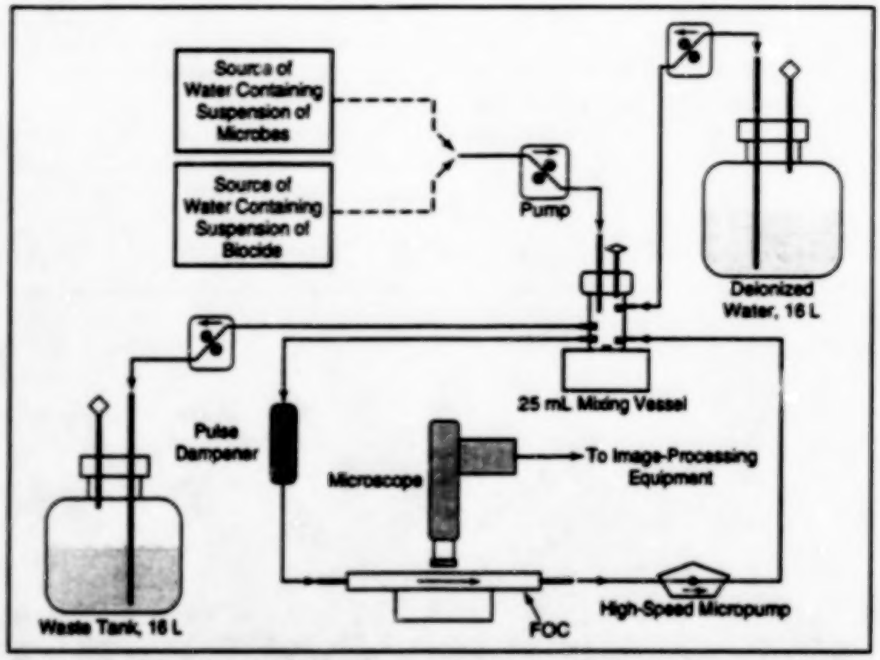

Figure 1. The Microscope and Video Camera generate images of water-borne microbes that have attached themselves to a solid surface. The images are digitized and processed to yield cell counts as a function of time.

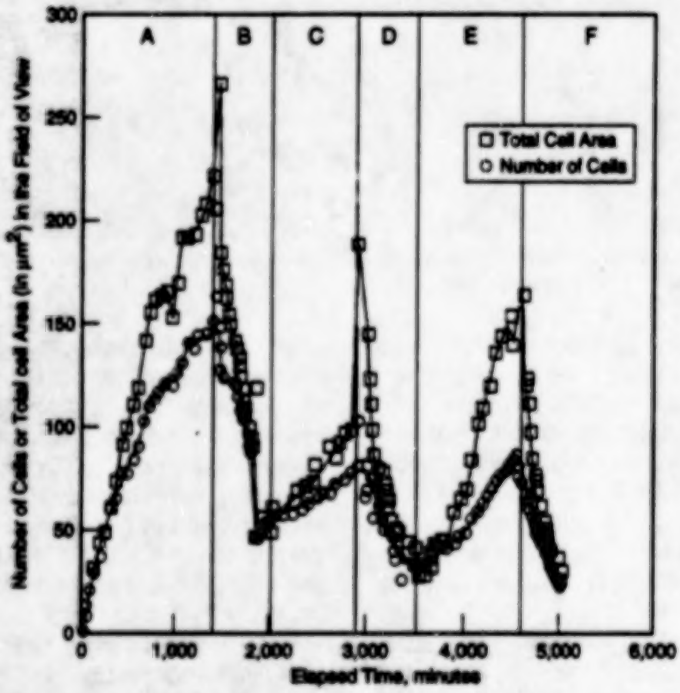

Plot	Phase of Experiment
A	Adhesion
B	Treatment With 12 ppm of Chlorine
C	Adhesion
D	Treatment With 24 ppm of Chlorine
E	Adhesion
F	Treatment With 48 ppm of Chlorine

Figure 2. These Plots of Cell Counts Versus Time were obtained in an experiment in which the microbes were *Pseudomonas capacia*.

recirculation loop with the high-speed micropump are isolated from the source of the cell suspension and washed with 300 mL of deionized water. Next, water containing the biocide to be tested is pumped into the FOC and recirculated through the FOC for 5 to 6 hours, during which time more images are analyzed and data collected. This is followed by another wash cycle, which is followed by another cycle of recirculation of the cell suspension and analysis of images, to measure the rate and degree of attachment on the surface of interest after the treatment with the biocide (see figure). Images are acquired at a frequency of at least once an hour, to measure the rate of attachment, and at least once every 20 minutes, to evaluate the effect of the biocide on the size of microbes and on the rate of detachment.

This work was done by Duane L. Pierson of **Johnson Space Center** *and David W. Koenig and Saroj K. Mishra of KRUG Life Sciences, Inc. Further information is contained in a TSP [see page 1].*

This invention is owned by NASA, and a patent application has been filed. Inquiries concerning nonexclusive or exclusive license for its commercial development should be addressed to the Patent Counsel, Johnson Space Center, (281) 483-0837. Refer to MSC-22679.

Device for Testing Susceptibility of Bacteria to Antibiotics

Tests can be performed safely, easily, and quickly.

Lyndon B. Johnson Space Center, Houston, Texas

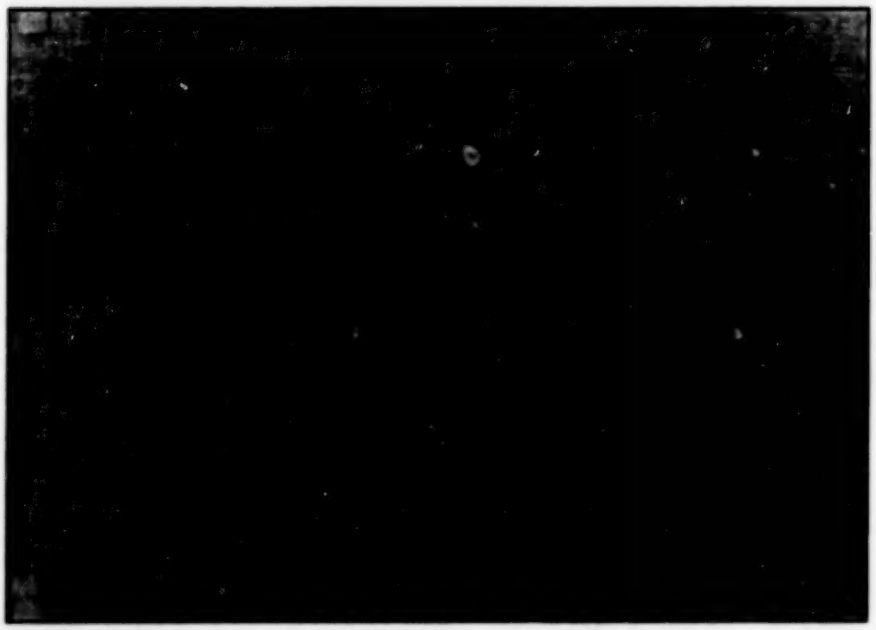

The Reaction Wells of This Device exhibit colors that were developed in a test of antibiotic substrates with *Staphylococcus aureus*.

A compact, lightweight, device makes it possible to assess the effects of antibiotics on bacteria. The device safely contains the antibiotic/bacteria mixtures, and its operation involves minimal ancillary equipment and minimal expense of time and effort by technicians. Originally designed for use aboard spacecraft, the device could also be mass-produced for use on Earth in isolated, remote environments and in situations in which automated instrumentation is inaccessible.

Testing to assess the effectiveness of antibiotics has been made necessary by the emergence of resistance to antibiotics in several common bacterial pathogens. Such testing is routinely performed in clinical laboratories by traditional manual and automated methods. An important measure of antibiotic effectiveness in laboratory testing is the highest dilution (minimum concentration) at which the drug under test inhibits the growth of bacteria; this concentration is known as the minimal inhibitory concentration (MIC). Using the present device, one can determine the MIC of an antibiotic with respect to the bacteria of interest, without the complex fluid-handling procedures and without the relatively bulky, expensive, power-consuming equipment of traditional laboratory testing.

The device is a modified version of a commercial test card that provides visual indications of MIC values. The card is credit-card-sized, weighs less than 15 grams, and contains 30 small reaction wells. The reaction wells are filled with dehydrated antibiotic substrates mixed with the antibiotics at various levels of dilution. The modification consists of the addition of Alamar Blue (a redox indicator) to the mixture in the reaction wells. This redox indicator serves as a visual indicator of the growth of bacteria in the wells. Resistance of microbes to the antibiotic in a given well is manifested by a distinctive bright pink color in the wells, whereas susceptibility of the microbes to the antibiotic is indicated by a blue color in that well.

To initiate a test, a technician inoculates the wells with a suspension of microbes that has been prepared from a 24-hour culture of the species of interest. The inoculated device is placed in a Ziploc (or equivalent) edge-sealing plastic bag and incubated at a temperature of 35 °C for 18 to 24 hours. After incubation, the device (see figure) is inspected and the colors in the wells are recorded.

In the original space-flight application, two devices are inoculated and bagged in a terrestrial laboratory. One device is transported under refrigeration at 4 °C, then incubated in the low-gravity test environment; another device that serves as a control is similarly refrigerated and incubated on Earth.

This work was done by Duane L. Pierson of **Johnson Space Center**, *Joyce A. Skweres and Saroj K. Mishra of KRUG Life Sciences, and James H. Jorgensen of UT-Health Science. Further information is contained in a TSP [see page 1].*

MSC-22658

Improved Unidirectional Cell-Stretching Device

Cells can be stretched controllably, without removing them from a culture medium.

Lyndon B. Johnson Space Center, Houston, Texas

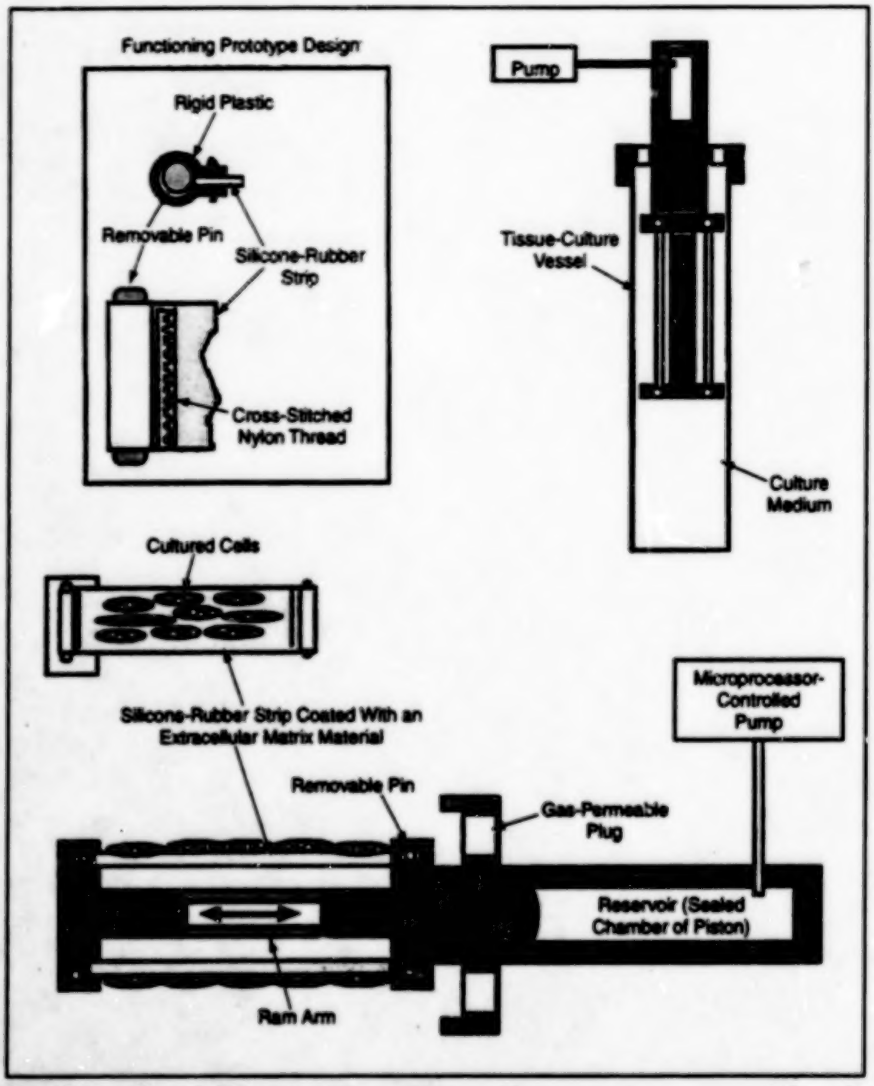

This Unidirectional Cell Stretcher incorporates several improvements over commercially available cell stretchers.

An improved stretching device has been developed for use in research on the effects of unidirectional loading on human and animal cells. The device is capable of applying or removing a load (a controlled amount of stretch) on command to mimic the loading or unloading experienced by skeletal muscles and other tissues of interest.

This device is designed to overcome the deficiencies of three cell-stretching devices that were commercially available at the time of reporting the information for this article. In the present device as in the commercial devices, a cell culture is grown on a coated sheet of silicone rubber that is immersed in a culture medium and the sheet is stretched to apply the desired load. One of the commercial devices can apply the load only in discrete steps and must be removed from the culture medium to change to a different load step. The other two commercial devices contain circular silicone membranes that are deformed in such ways that the resulting stretches include radial components and are thus not the desired unidirectional stretches. The present device need not be removed from the culture medium and produces a continuously adjustable, truly unidirectional stretch.

The silicone rubber sheets in the present device are in the form of rectangular strips coated with an extracellular matrix compound (i.e., collagen Type I). The strips are arranged parallel to each other, with their long axes laid out along the axis of a round cylindrical ram (see figure). By use of removable pins, the ends of the strips are attached to the ends of the ram at equal circumferential intervals. This design makes it possible to grow cells on the strips in standard tissue culture plates to the required cell density or differentiation state before placing the strip in the cell stretcher. This design also offers the advantage of ease of removal of the cells for examination at the end of the stretching procedure.

The ram assembly with the strips attached is inserted in a tissue-culture vessel that contains a culture medium. The stretching actuator in the ram is a sealed-chamber piston. Stretching along the cylindrical axis is effected by injection of a sterile fluid into the sealed chamber by use of a pump controlled by a microprocessor. (The pump is situated outside the culture vessel.) Reversal of the injection flow results in a decrease in the amount of stretch. The rate of stretching or unstretching is controlled by controlling the rate of flow.

According to a proposed alternative design of this device, the ram would be advanced by a screw drive actuated by a microprocessor-controlled stepping motor. According to another proposed alternative design, the cell stretcher would be built into a tissue-culture vessel that would include a heater, a temperature sensor, ports for exchange and/or sampling of the culture medium, a port for infusion of gas, a pressure sensor, gas sensors, and optical ports for observation of cells during the loading procedure.

This work was done by Daniel L. Feeback of **Johnson Space Center** *and Mark S. F. Clarke of the National Research Council. Further information is contained in a TSP [see page 1].*

This invention is owned by NASA, and a patent application has been filed. Inquiries concerning nonexclusive or exclusive license for its commercial development should be addressed to the Patent Counsel, Johnson Space Center, (281) 483-0837. Refer to MSC-22834.

END

10-5-00